

1  
2  
3  
4  
5  
6  
7  
8  
9  
10  
11  
12  
13  
14  
15  
16  
17  
18  
19  
20  
21  
22  
23  
24  
25

**High-resolution regional emission inventory contributes to  
the evaluation of policy effectiveness: A case study in Jiangsu  
province, China**

Chen Gu<sup>1</sup>, Lei Zhang<sup>1,2</sup>, Zidie Xu<sup>1</sup>, Sijia Xia<sup>3</sup>, Yutong Wang<sup>1</sup>, Li Li<sup>3</sup>, Zeren Wang<sup>1</sup>,  
Qiuyue Zhao<sup>3</sup>, Hanying Wang<sup>1</sup>, Yu Zhao<sup>1,2\*</sup>

<sup>1</sup> State Key Laboratory of Pollution Control and Resource Reuse and School of the Environment, Nanjing University, 163 Xianlin Rd., Nanjing, Jiangsu 210023, China

<sup>2</sup> Collaborative Innovation Center of Atmospheric Environment and Equipment Technology, CICAET, Nanjing, Jiangsu 210044, China

<sup>3</sup> Jiangsu Key Laboratory of Environmental Engineering, Jiangsu Provincial Academy of Environmental Sciences, Nanjing, Jiangsu 210036, China

\*Corresponding author: Yu Zhao

Phone: 86-25-89680650; email: [yuzhao@nju.edu.cn](mailto:yuzhao@nju.edu.cn)

## 26 Abstract

27 China has been conducting a series of actions on air quality improvement for the past  
28 decades, and air pollutant emissions have been changing swiftly across the country.  
29 Province is an important administrative unit for air quality management in China, thus  
30 reliable provincial-level emission inventory for multiple years is essential for  
31 detecting the varying sources of pollution and evaluating the effectiveness of emission  
32 controls. In this study, we selected Jiangsu, one of the most developed provinces in  
33 China, and developed the high-resolution emission inventory of nine species for  
34 2015-2019, with improved methodologies for different emission sectors, best  
35 available facility-level information on individual sources, and real-world emission  
36 measurements. Resulting from implementation of strict emission control measures,  
37 the anthropogenic emissions were estimated to have declined 53%, 20%, 7%, 2%,  
38 10%, 21%, 16%, 6% and 18% for sulfur dioxide (SO<sub>2</sub>), nitrogen oxides (NO<sub>x</sub>),  
39 carbon monoxide (CO), non-methane volatile organic compounds (NMVOCs),  
40 ammonia (NH<sub>3</sub>), inhalable particulate matter (PM<sub>10</sub>), fine particulate matter (PM<sub>2.5</sub>),  
41 black carbon (BC), and organic carbon (OC) from 2015 to 2019, respectively. Larger  
42 abatement of SO<sub>2</sub>, NO<sub>x</sub> and PM<sub>2.5</sub> emissions were detected for the more developed  
43 southern Jiangsu. Since 2016, the ratio of biogenic volatile organic compounds  
44 (BVOCs) to anthropogenic volatile organic compounds (AVOCs) exceeded 50% in  
45 July, indicating the importance of biogenic sources on summer O<sub>3</sub> formation. Our  
46 estimates in annual emissions of NO<sub>x</sub>, NMVOCs, and NH<sub>3</sub> were generally smaller  
47 than the national emission inventory MEIC, but larger for primary particles. The  
48 discrepancies between studies resulted mainly from different methods of emission  
49 estimation (e.g., the procedure-based approach for AVOCs emissions from key  
50 industries used in this work) and inconsistent information of emission source  
51 operation (e.g., the penetrations and removal efficiencies of air pollution control  
52 devices). Regarding the different periods, more reduction of SO<sub>2</sub> emissions was found  
53 between 2015 and 2017, ~~and of~~ NO<sub>x</sub>, AVOCs and PM<sub>2.5</sub> between 2017 and 2019.  
54 Among the selected 13 major measures, the ultra-low emission retrofit on power

删除的内容: but

56 sector was the most important contributor to the reduced SO<sub>2</sub> and NO<sub>x</sub> emissions  
57 (accounting for 38% and 43% of the emission abatement, respectively) for 2015-2017,  
58 but its effect became very limited afterwards as the retrofit had been commonly  
59 completed by 2017. Instead, extensive management of coal-fired boilers and  
60 upgradation and renovation of non-electrical industry were the most important  
61 measures for 2017-2019, accounted collectively for 61%, 49% and 57% reduction of  
62 SO<sub>2</sub>, NO<sub>x</sub> and PM<sub>2.5</sub>, respectively. Controls on key industrial sectors maintained the  
63 most effective for AVOCs reduction for the two periods, while measures on other  
64 sources (transportation and solvent replacement) became more important for recent  
65 years. Our provincial emission inventory was demonstrated to be supportive for  
66 high-resolution air quality modeling for multiple years. Through scenario setting and  
67 modeling, worsened meteorological conditions were found from 2015 to 2019 for  
68 PM<sub>2.5</sub> and O<sub>3</sub> pollution alleviation. However, the efforts on emission controls were  
69 identified to largely overcome the negative influence of meteorological variation. The  
70 changed anthropogenic emissions were estimated to contribute 4.3 and 5.5 μg·m<sup>-3</sup> of  
71 PM<sub>2.5</sub> concentration reduction for 2015-2017 and 2017-2019, respectively. While  
72 elevated O<sub>3</sub> by 4.9 μg·m<sup>-3</sup> for 2015-2017, the changing emissions led to 3.1 μg·m<sup>-3</sup> of  
73 reduction for 2017-2019, partly (not fully though) offsetting the meteorology-driven  
74 growth. The analysis justified the validity of local emission control efforts on air  
75 quality improvement, and provided scientific basis to formulate air pollution  
76 prevention and control policies for other developed regions in China and worldwide.

## 77 **1. Introduction**

78 Severe air pollution is of great concern for fast industrialized countries like China,  
79 especially in economically developed regions where an overlap of serious pollution  
80 levels and dense populations has resulted in high exposure and adverse health  
81 outcomes (Klimont et al., 2013; Hoesly et al., 2018). Emission inventory, which  
82 contains complete information on the magnitude, spatial pattern, and temporal change  
83 of air pollutant emissions by sector, is essential for identifying the sources of air

84 pollution and effectiveness of emission controls on air quality through numerical  
85 modeling (Zhao et al., 2013). Improving the understanding of emission behaviors and  
86 reducing the uncertainty of emission estimates have always been the main focus of  
87 emission inventory studies, given the big variety of source categories, fast changing  
88 mix of manufacturing and emission control technologies, and insufficient  
89 measurements of real-world emissions. At the global and continental scales, emission  
90 inventories have been developed by combining available information of large point  
91 sources and improved surrogate statistics for area sources, e.g., Emissions Database  
92 for Global Atmospheric Research (EDGAR, <https://edgar.jrc.ec.europa.eu/>, Crippa et  
93 al., 2020) and Regional Emission Inventory in Asia (REAS,  
94 <https://www.nies.go.jp/REAS/>, Kurokawa et al., 2020). As the largest developing  
95 country in the world, China has been proven to contribute greatly to global emissions  
96 (Klimont et al., 2013; Huang et al., 2014; Wiedinmyer et al., 2014; Miyazaki et al.,  
97 2017).

98 Along with the improved methodology and increasing availability of emission source  
99 and field measurement data, the applicability and reliability of recent Chinese  
100 emission inventories (e.g., the Multi-resolution Emission Inventory for China, MEIC,  
101 Zheng et al., 2018) have been considerably improved compared to the earlier  
102 large-scale studies for Asia or the world. When the research focus switches to smaller  
103 provincial and city scales, the uncertainty of national emission inventory may increase  
104 attributed mainly to the insufficient information on detailed emission sources,  
105 particularly for medium/small size stationary and area sources. Certain “proxies”  
106 including population and economic densities were commonly applied to downscale  
107 the emissions from coarser to finer horizontal resolution, based on the assumption that  
108 those proxies were strongly associated with emission intensity. Such “coupling effect”,  
109 however, has been demonstrated to be weakened for recent years. For example, a  
110 great number of big industrial facilities have been gradually moved out of urban  
111 centers, resulting in an inconsistency between emission and population hotspots.  
112 Therefore, inappropriate application of those proxies could lead to great uncertainty in  
113 emission estimation and thereby enhanced bias in air quality modeling (Zhou et al.,

114 2017; Zheng et al., 2017). For the urgent demand for preventing regional air pollution  
115 and relevant health damage, therefore, development of high-resolution emission  
116 inventories has been getting essential, especially in regions with developed industry,  
117 large population and complex emission sources (Zheng et al., 2009; Shen et al., 2017;  
118 Zhao et al., 2018). With increased proportion of point sources and more complete  
119 facility-based information, the improved emission inventory could reduce the  
120 arbitrary use of proxy-based downscaling technique and thereby the uncertainty of the  
121 emission estimates (Zhao et al., 2015; Zheng et al., 2021).

122 For the past decade, China has been conducting a series of actions to tackle the  
123 serious air pollution problem. With the mitigation of severe fine particulate matter  
124 ( $PM_{2.5}$ ) pollution set as a priority from 2013 to 2017, the National Action Plan on Air  
125 Pollution Control and Prevention (NAPAPCP, State Council of the People's Republic  
126 of China (SCC), 2013) pushed stringent end-of-pipe emission controls (e.g., the  
127 "ultra-low" emission control for power sector) and retirement of small and  
128 energy-inefficient factories (Zhang et al., 2019a; 2019b; Zheng et al., 2018). On top of  
129 that, China announced the "Three-Year Action Plan to Fight Air Pollution"  
130 (TYAPFAP) to further reduce  $PM_{2.5}$  and ozone ( $O_3$ ) levels for 2018-2020 (SCC, 2018).  
131 Substantially enhanced measures have been required for reducing industrial (e.g.,  
132 application of "ultra-low" emission control for selected non-electrical industries) and  
133 residential emissions (e.g., promotion of advanced stoves and clean coal during  
134 heating seasons). Those measures have changed the air pollutant emissions and  
135 thereby air quality over the country. Studies have been conducted to assess the  
136 contribution of the nation actions to the improvement of air quality, based usually on  
137 the national emission inventory. For example, Zhang et al. (2019a) estimated a  
138 nationwide 30-40% reduction in  $PM_{2.5}$  concentration attributed to NAPAPCP from  
139 2013 to 2017.

140 Province is an important administrative unit for air quality management in China.  
141 Given the heterogeneous economical and energy structures as well as atmospheric  
142 conditions, there are usually big diversities in the strategies and actions of reducing  
143 regional air pollution adopted by the local governments, leading to various progresses

144 of emission and air quality changes (Liu et al., 2022; Wang et al., 2021a). Limited by  
145 incomplete or inconsecutive information on emission sources and lack of on-time  
146 emission measurements, however, there were few studies on provincial-level emission  
147 inventories for multiple years. Studies based on the national emission inventories  
148 would be less supportive for policy makers to formulate the emission control  
149 measures and to evaluate their effectiveness on emission reduction and air quality  
150 improvement (An et al., 2021; Huang et al., 2021). Contrary to NAPAPCP that has  
151 been noticed, moreover, few analyses have been conducted for TYAPFAP after 2017  
152 due partly to lack of most recent emission data, preventing comparison and  
153 comprehensive understanding of the effectiveness of emission controls for the two  
154 phases. Jiangsu Province, located on the northeast coast of the Yangtze River Delta  
155 region (YRD), is one of China's most industrial developed and heavy-polluted regions.  
156 It contributed to 10.1% of the gross domestic product (GDP) in mainland China  
157 (ranking the second place in the country), and 6.4%, 11.3% and 11.4% of national  
158 cement, pig iron and crude steel production in 2020, respectively (National Bureau of  
159 Statistics of China, 2021). MEIC indicated the emissions per unit area of  
160 anthropogenic sulfur dioxide (SO<sub>2</sub>), nitrogen oxides (NO<sub>x</sub>), non-methane volatile  
161 organic compounds (NMVOCs), PM<sub>2.5</sub>, and ammonia (NH<sub>3</sub>) in Jiangsu were 2.8, 6.5,  
162 7.0, 4.5 and 4.8 times of the national average in 2017, respectively. Resulting from the  
163 implementation of air pollution prevention measures, PM<sub>2.5</sub> pollution in Jiangsu has  
164 been alleviated since 2013, while the great changes in emissions due to varying  
165 energy use and industry and transportation development have made it the province  
166 with the highest O<sub>3</sub> concentration and the fastest growth rate of O<sub>3</sub> in YRD for recent  
167 years (Zheng et al., 2016; Wang et al., 2017; Zhang et al., 2017a; Zhou et al., 2017).  
168 In this study, therefore, we took Jiangsu as an example to demonstrate the  
169 development of high-resolution emission inventory and its application on evaluating  
170 the effectiveness of emission control actions. We integrated the methodological  
171 improvements on regional emission inventory by our previous studies (Zhou et al.,  
172 2017; Zhao et al., 2017; 2020; Wu et al., 2022; Zhang et al., 2019b; Zhang et al., 2020;  
173 2021b), and compiled and incorporated best available facility-level information and

174 real-world emission measurements (see details in the methodology and data section).  
175 A provincial-level emission inventory for 2015-2019 was then thoroughly developed  
176 for nine gaseous and particulate species (SO<sub>2</sub>, NO<sub>x</sub>, NMVOCs, carbon dioxide (CO),  
177 inhalable particulate matter (PM<sub>10</sub>), PM<sub>2.5</sub>, NH<sub>3</sub>, black carbon (BC), and organic  
178 carbon (OC)). The difference between our emission inventory and others, as well as  
179 its main causes, was carefully explored. Using a measure-specific integrated  
180 evaluation approach, we further identified the drivers of emission changes of SO<sub>2</sub>,  
181 NO<sub>x</sub>, PM<sub>2.5</sub> and anthropogenic volatile organic compounds (AVOCs), with an  
182 emphasis on the impacts of 13 major control measures summarized from NAPAPCP  
183 and TYAPFAP. Finally, air quality modeling was applied to assess the reliability of  
184 our emission inventory and to quantify the contribution of emission controls to the  
185 changing PM<sub>2.5</sub> and O<sub>3</sub> concentrations for 2015-2017 within NAPAPCP and  
186 2017-2019 within TYAPFAP, and the differentiated impacts of emission controls on  
187 air quality were revealed for the two phases.

## 188 **2. Methodology and data**

### 189 **2.1 Emission estimation**

#### 190 **2.1.1 Emission source classification**

191 We applied a four-level framework of emission source categories for Jiangsu emission  
192 inventory, based on a thorough investigation on the energy and industrial structures in  
193 the province. The framework included six first-level categories, covering all the social  
194 and economic sectors in Jiangsu: power sector, industry, transportation, agriculture,  
195 residential, and biogenic source (for NMVOCs only). Moreover, the framework  
196 contained 55 second-level categories based on facility/equipment types and  
197 economical subsectors, 240 third-level categories classified mainly by fuel, product,  
198 and material types, and a total of 870 fourth-level categories including sources by  
199 combustion, manufacturing and emission control technologies of emission facilities  
200 (details on the first three level sectors are listed in Table S1 in the Supplement).

删除的内容: this study

202 Compared to the guidelines of national emission inventory development (He et al.,  
203 2018), 42 new categories (third-level) were added in this study, contained mainly in  
204 the second-level categories including metal products and the mechanical equipment  
205 manufacturing industries, non-industrial solvent usage from ship fittings and repairs,  
206 household appliances, and housing retrofitting emissions. Those categories were  
207 identified as important sources of NMVOCs emissions in Jiangsu. In particular, ship  
208 coating emissions, coming mainly from solvent usage during spraying, cleaning and  
209 gluing in a wide range of procedures, could account for nearly 20% of the solvent use  
210 emissions in the YRD region (Mo et al., 2021). Therefore, the updated framework  
211 provides a more complete coverage of source categories, thus considerably reduces  
212 the bias of emission estimation due to missing potentially important emitters.

### 213 **2.1.2 Emission estimation methods**

214 We applied the “bottom-up” methodology (i.e., the emissions were calculated at the  
215 finest source level (e.g., facility level if data allowed) and then aggregated to upper  
216 categories/regions) to develop the high-resolution emission inventory for Jiangsu (and  
217 its 13 cities, as shown in Figure S1 in the Supplement) 2015-2019. As mentioned in  
218 Introduction, we have conducted a series of studies and made substantial  
219 improvements on the methodology of regional emission inventory development by  
220 source category or species, compared to the ones at larger spatial scales. Here we  
221 integrated those improvements as briefly described below, and additional further  
222 details can be found in corresponding published articles.

223 **Power plant** We developed a method of examining, screening and applying online  
224 measurement data from the continuous emission monitoring systems (CEMS, Zhang  
225 et al., 2019b) to estimate the emissions at the power unit/plant level. For units without  
226 CEMS data, we applied the average flue gas concentrations obtained from CEMS for  
227 units with the same installed capacity. The emissions were calculated based on the  
228 annual mean hourly flue gas concentration of air pollutant obtained from CEMS and  
229 the theoretical annual flue gas volume of each unit/plant:



230 
$$E_{i,j} = C_{i,j} \times AL_j \times V_m^0 \quad (1)$$

231 where  $E$  is the emission of air pollutant;  $i$ ,  $j$  and  $m$  represent the pollutant species,  
232 individual plant/unit, and fuel type, respectively;  $C$  is the annual average  
233 concentration in the flue gas;  $AL$  is the annual coal consumption, and  $V^0$  is the  
234 theoretical flue gas volume per unit of fuel consumption, which depends on the coal  
235 type and can be calculated following the method in Zhao et al. (2010).

236 **Industrial plant** Emissions were principally calculated based on activity level data  
237 (production output or energy consumption) and emission factor (emissions per unit of  
238 activity level). For point sources with abundant information, we used a  
239 procedure-based approach to calculate the emissions of pollutants (Zhao et al., 2017).  
240 For example, we subdivided the iron and steel industry into sintering, pelletizing, iron  
241 making, steel making, rolling steel, and coking. The activity data and emission factors  
242 of each procedure were derived based on multiple information collected from  
243 enterprise regular report, statistics, and/or on-site investigation at the facility level (see  
244 Section 2.1.3). The emissions of air pollutants were calculated using Eq. (2):

245 
$$E_i = \sum_{j,r} AL_{j,r} \times EF_{i,j,r} \times (1 - \eta_{i,j,r}) \quad (2)$$

246 where  $r$  is the industrial procedure;  $AL$  is the activity level;  $EF$  is the unabated  
247 emission factor;  $\eta$  is the pollutant removal efficiency of end-of-pipe control  
248 equipment.

249 **Petrochemical industry** Certain procedures in petrochemical industry have been  
250 identified as the main contributors to AVOCs emissions from the sector. For example,  
251 equipment leaks, storage tanks, and manufacturing lines were estimated to be  
252 responsible for over 90% of the total emissions (Ke et al., 2020; Liu et al., 2020; Yen  
253 and Horng, 2009). Through field measurements and in-depth analysis of different  
254 emission calculation methods, Zhang et al. (2021a) suggested that procedure-based  
255 method should provide better estimate of NMVOCs emissions for petroleum  
256 industries than the commonly approach that applied a full emission factor for the  
257 whole factory. In this study, therefore, we applied the procedure-based method for  
258 four key procedures (manufacturing lines, storage tanks, equipment leaks, and

259 wastewater collection and treatment system), with best available information from  
260 on-site surveys and regular enterprise reports.

261 | **Agriculture** Agricultural NH<sub>3</sub> emissions can be influenced by the meteorology, soil  
262 environment, farming manners, and thus are more difficult to track compared to SO<sub>2</sub>  
263 and NO<sub>x</sub> that are commonly from power and industrial plants. For example, high  
264 temperature and top-dressing fertilization conducted in summer could elevate NH<sub>3</sub>  
265 volatilization from urea fertilizer uses in YRD. Our previous work (Zhao et al., 2020)  
266 quantified the effects of meteorology, soil property and various agricultural processes  
267 (e.g., fertilizer use and manure management) on YRD NH<sub>3</sub> emissions for 2014. Here  
268 we expanded the research period and obtained the agricultural NH<sub>3</sub> emission  
269 inventory for 2015-2019 in Jiangsu.

270 **Off-road transportation** In this work, we combined the method developed by Zhang  
271 et al. (2020) and newly tested emission factors to estimate the emissions from off-road  
272 machines in Jiangsu for multiple years. We developed a novel method to estimate the  
273 emissions and their spatiotemporal distribution for in-use agricultural machinery, by  
274 combining satellite data, land and soil information, and in-house investigation (Zhang  
275 et al., 2020). In particular, the machinery usage was determined based on the spatial  
276 distribution, growing and rotation pattern of the crops. Moreover, twelve construction  
277 and agricultural machines with different power capacity and emission grades (China  
278 I-III) were selected and emission factors were measured under various working loads  
279 (unpublished).

280 **Biogenic source:** Located in the subtropics, Jiangsu has abundant broadleaf  
281 vegetation, a main contributor to biogenic volatile organic compounds (BVOCs)  
282 emissions. Our previous work (Wang et al., 2020b) evaluated the effect of land cover  
283 data, emission factors and O<sub>3</sub> exposure on BVOCs emissions in YRD with the Model  
284 of Emissions of Gases and Aerosols from Nature (MEGAN). Here we followed the  
285 improved method by Wang et al. (2020b) and calculated BVOCs emissions with  
286 integrated land cover information, local BVOCs emission factors, and influence of  
287 actual O<sub>3</sub> stress in Jiangsu.

288 **Other sources** Emissions from on-road vehicles and residential sectors were

删除的内容: greatly

290 estimated following our previous work (Zhou et al., 2017; Zhao et al., 2021), with  
291 updated activity levels and emission factors.

292 **NMVOCs speciation** We updated NMVOCs speciation by incorporating the local  
293 source profiles from field measures (Zhao et al., 2017; Zhang et al., 2021a) and  
294 massive literature reviews of previous studies (Mo et al., 2016; Li et al., 2014; Huang  
295 et al., 2021; Wang et al., 2020a). Compared with the widely used SPECIATE 4.4  
296 database (<https://www.epa.gov/air-emissions-modeling/speciate>, Hsu et al., 2018), we  
297 included new source profiles from local measurements for production of sugar,  
298 vegetable oil and beer, and refined the source profiles for the use of paints, inks,  
299 coatings, dyes, dyestuffs and adhesives in manufacturing industry (Zhang et al.,  
300 2021a), and selected production processes of chemical engineering (Zhao et al., 2017).  
301 Moreover, we applied more detailed profiles for some finer categories compared to  
302 the coarser source categories in the guidelines of national emission inventory  
303 development. for example, NMVOCs release during filling into petrol and diesel  
304 release, metal surface treatment into water-based and solvent-based paints, and ink  
305 printing into offset, gravure and letterpress printing. Those efforts made the NMVOCs  
306 speciation more representative for local emission sources (Zhang et al., 2021a).

### 307 **2.1.3 Data compilation, investigation and incorporation**

308 In this study, we compiled, investigated and incorporated most available information  
309 on emission sources to improve the completeness, representativeness and reliability of  
310 provincial emission inventory. In particular, we collected officially reported  
311 Environmental Statistics Database (ESD, 2015-2019) and the Second National  
312 Pollution Source Census (SNPSC, 2017) for stationary sources (mostly power and  
313 industrial ones). Both of them contained basic information on their location, raw  
314 material and energy consumption, product output, and manufacturing and emission  
315 control technologies. The former database was routinely reported for relatively big  
316 point sources every year, but some information could be outdated or inaccurate  
317 attributed to insufficient on-site inspection. Through wide on-site surveys, in contrast,

删除的内容: .

删除的内容: For

删除的内容: in

删除的内容: station

322 the latter database included much more plants, and provided or corrected crucial  
323 information at facility level, such as removal efficiency of air pollutant control  
324 devices (APCD). However, the database was developed for 2017 and could not track  
325 the changes for recent years. Therefore, we further applied an internal database from  
326 the Air Pollution Source Emission Inventory Compilation and Analysis System  
327 (APSEICAS, <http://123.127.175.61:31000>), which was developed by Jiangsu  
328 Provincial Academy of Environmental Sciences. Following the principal of SNPSC,  
329 the information of APSEICAS has been collected and dynamically updated since 2018,  
330 based mainly on in-depth investigation for individual enterprises conducted jointly by  
331 themselves and local environmental administrators. We made cross validation and  
332 necessary revision according to above-mentioned three databases, to ensure the  
333 accuracy of information as much as possible.

334 As a result, we obtained sufficient numbers of point sources with satisfying  
335 facility-level information for provincial-level emission inventory development  
336 (57,457, 32,324 and 48,826 for 2017, 2018, and 2019, respectively). The shares of  
337 coal consumption by those sources to the total ranged 90-94% for the three years. The  
338 high proportions of point sources could effectively reduce the uncertainty in  
339 estimation and spatial allocation of air pollutant emissions. For the remaining  
340 industrial sources, the emissions were calculated by using the average emission factor  
341 of each sector in each city, and were spatially allocated according to the distribution of  
342 local industrial parks and GDP data extracted from a database of the Chinese  
343 Academy of Sciences (CAS) for 2015 at a horizontal resolution of 1 km  
344 (<https://www.resdc.cn/DOI/DOI.aspx?DOIid=33>).

345 Other information on area industrial sources, transportation, agricultural, and  
346 residential sources were taken from economical and energy statistical yearbooks at  
347 city level. Activity data that were not recorded (e.g., civil solvent usage, catering, and  
348 biomass burning) were indirectly estimated from relevant statistics, including  
349 population, building area, and crop yields.

## 350 **2.2 Analysis of emission change**

351 In this study, we summarized 13 major control measures adopted between 2015 and  
352 2019, based on NAPAPCP, TYAPFAP and relative action plans promulgated by the  
353 Jiangsu government (Figure S2 in the Supplement). Those included 1) ultra-low  
354 emission retrofit of coal-fired power plants, 2) extensive management of coal-fired  
355 boilers, 3) upgradation and renovation of non-electrical industry, 4) phasing out  
356 outdated industrial capacities, 5) promoting clean energy use, 6) phasing out small  
357 polluting factories, 7) construction of port shore power, 8) comprehensive treatment  
358 of mobile source pollution, 9) VOCs emission control in key sectors, 10) application  
359 of leak detection and repair (LDAR), 11) oil and gas recovery, 12) replacement with  
360 low-VOC paints, 13) control of non-point pollution. We applied the method by Zhang  
361 et al. (2019a) to quantify the benefits of those air clean actions on emission abatement.  
362 Briefly, the emission reduction resulting from the implementation of a specific  
363 measure was estimated by changing the parameters of emission calculation associated  
364 with the measure within the concerned period, and keeping other parameters constant  
365 (same as initial year). The emission reduction from each measure was then estimated  
366 for 2015-2017 and 2017-2019. The provincial-level emission inventory developed in  
367 Section 2.1 was adopted as the baseline of the emission estimates. It is worth noting  
368 that the aggregated emission reduction from all the measures is not equal to the actual  
369 reduction, as the factors leading to emission growth were not counted in this analysis.

## 370 **2.3 Air quality modeling**

### 371 **2.3.1 Model configurations**

372 To evaluate the provincial-level emission inventory, we used the Community  
373 Multiscale Air Quality (CMAQ v5.1) model developed by US Environmental  
374 Protection Agency (USEPA), to simulate the PM<sub>2.5</sub> and O<sub>3</sub> concentrations in Jiangsu.  
375 Four months representing the four seasons (January, April, July, and October) of each  
376 year between 2015 and 2019 were selected as the simulation periods, with a spin-up

删除的内容: are selected to

378 time of 7 days for each month to reduce the impact of the initial condition on the  
379 simulation. As shown in Figure S1, three nested domains (D1, D2, and D3) were  
380 applied with the horizontal resolutions of 27, 9, and 3 km, respectively, and the most  
381 inner D3 covered Jiangsu and parts of the YRD region including Shanghai, northern  
382 Zhejiang, and eastern Anhui. MEIC was applied for D1, D2, and the regions out of  
383 Jiangsu in D3, and the provincial-level emission inventory was applied for Jiangsu in  
384 D3. The emission data outside Jiangsu in D3 were originally from MEIC and  
385 downscaled to the resolution of 3km×3km with the "proxy-based" approach. The  
386 Carbon Bond Mechanism (CB05) and AERO5 mechanisms were used for the  
387 gas-phase chemistry and aerosol module, respectively.

388 The meteorological field for the CMAQ model was obtained from the Weather  
389 Research and Forecasting model (WRF v3.4). Meteorological initial and boundary  
390 conditions were obtained from the National Centers for Environmental Prediction  
391 (NCEP) datasets for the assimilation in simulations. Ground observations at 3-h  
392 intervals were downloaded from National Climatic Data Center (NCDC) to evaluate  
393 the WRF modelling performance, and statistical indicators including bias, index of  
394 agreement (IOA), and root mean squared error (RMSE) were calculated (Yang et al.,  
395 2021a). The discrepancies between simulations and ground observations were within  
396 an acceptable range (Table S2 in the Supplement).

397 In order to evaluate the model performance of CMAQ, we collected ground  
398 observation data of hourly PM<sub>2.5</sub> and O<sub>3</sub> concentrations at the 110 state-operating air  
399 quality monitoring stations within Jiangsu (<https://data.epmap.org/page/index>, see the  
400 station locations in Figure S1). Correlation coefficients (R), normalized mean bias  
401 (NMB) and normalized mean errors (NME) between observation and simulation for  
402 each month were calculated to evaluate the performance of CMAQ modeling:

$$403 \quad NMB = \frac{\sum_{p=1}^n (S_p - O_p)}{\sum_{p=1}^n O_p} \times 100\% \quad (3)$$

$$404 \quad NME = \frac{\sum_{p=1}^n |S_p - O_p|}{\sum_{p=1}^n O_p} \times 100\% \quad (4)$$

405 where  $S_p$  and  $O_p$  are the simulated and observed concentration of air pollutant,  
406 respectively, and  $n$  indicates the number of available data pairs.

407 We further compared the modeling performance using provincial-level emission  
408 inventory in D3 with that using MEIC in D2. Basically, the proxies of total population  
409 and GDP were poorly correlated with gridded emissions dominated by point sources,  
410 and the proxy-based methodology would result in great uncertainty in downscaling  
411 emissions and thereby air quality modeling from coarser to finer resolution. For  
412 example, Zheng et al. (2017) suggested a much larger bias for high-resolution  
413 simulation (additional 8-73% at 4 km) than that at coarser resolution (3-13% for 36  
414 km) when MEIC was applied in predicting surface concentrations of different air  
415 pollutants. Our previous work in YRD also demonstrated that downscaling national  
416 emission inventory with the proxy-based method resulted in clearly larger bias in  
417 high-resolution (3 km) air quality modeling than the provincial-level emission  
418 inventory with more point sources included (Zhou et al., 2017). To avoid expanding  
419 the modeling bias, therefore, we did not directly downscale MEIC into the entire D3,  
420 and the improvement of provincial emission inventory could be demonstrated with  
421 better model performance (in D3) than MEIC (in D2).

### 422 **2.3.2 Emission and meteorological factors affecting the variation of PM<sub>2.5</sub> and O<sub>3</sub>**

423 Besides the baseline simulations conducted for 2015, 2017, and 2019, we set up two  
424 extra scenarios, the meteorological variation (VMET) and the anthropogenic emission  
425 variation (VEMIS), to assess the impacts of emission and meteorological changes on  
426 the interannual variations of PM<sub>2.5</sub> and O<sub>3</sub> concentrations, and to reveal their varying  
427 contributions for different periods, as summarized in Table S3 in the supplement.  
428 VMET used the varying meteorological fields for the three years but fixed the  
429 emission input at the 2017 level, and was thus able to quantify the impact of changing  
430 meteorological conditions on PM<sub>2.5</sub> and O<sub>3</sub> concentrations. For example, the  
431 difference between 2015 and 2017 in VMET indicated the contribution of changing  
432 meteorology to variation of air pollutant concentration. Similarly, the emission  
433 variation scenario (VEMIS) used the varying emission inventory for the three years  
434 but fixed meteorological fields at the 2017 level, and was thus able to quantify the

删除的内容: one

436 impact of changing emissions on PM<sub>2.5</sub> and O<sub>3</sub> concentrations. The contributions  
437 between 2015 and 2017, and those between 2017 and 2019, could then be compared  
438 to evaluate the effectiveness of emission control on air quality for the two periods.  
439 Notably the anthropogenic emission change in the modeling scenario referred to that  
440 for entire D3, and thus the contribution of emission control to the changing air quality  
441 was from both Jiangsu and nearby regions. Given the clearly larger emission intensity  
442 for the former compared to the latter (An et al., 2021), the contribution of local  
443 emissions was expected to be more important on the air quality than regional transport.  
444 Moreover, the BVOCs emissions were selected in accordance with the used  
445 meteorological field for the given year, thus the interannual changes of BVOCs  
446 emissions were counted in the contribution of changing meteorology.

### 447 **3. Results and discussions**

#### 448 **3.1 Air pollutant emissions by sector and region**

##### 449 **3.1.1 Anthropogenic emissions by sector and their changes**

450 From 2015 to 2019, the total emissions of anthropogenic SO<sub>2</sub>, NO<sub>x</sub>, AVOCs, NH<sub>3</sub>,  
451 CO, PM<sub>10</sub>, PM<sub>2.5</sub>, BC, and OC in Jiangsu were estimated to decline 53%, 20%, 6%,  
452 10%, 7%, 21%, 16%, 6% and 18%, down to 296, 1122, 1271, 422, 7163, 565, 411, 32,  
453 and 36 Gg in 2019, respectively (Table S4 in the Supplement). On top of SO<sub>2</sub> and  
454 NO<sub>x</sub>, NMVOCs has been incorporated into national economic and social  
455 development plans with emission reduction targets in China since 2015, because of its  
456 harmful impact on human health and important role on triggering O<sub>3</sub> formation. The  
457 central government required the total national emissions of SO<sub>2</sub>, NO<sub>x</sub>, and AVOCs to  
458 be cut by 15%, 15%, and 10% during the 13th Five-Year Plan period (2015-2020),  
459 respectively (Zhang et al., 2022). Our estimates show that the actual SO<sub>2</sub> and NO<sub>x</sub>  
460 emission reductions were larger than planned in Jiangsu, due to the implementation of  
461 stringent pollution control measures. However, AVOCs emissions did not decline  
462 considerably within the research period, resulting from less penetration of efficient



463 APCD, and more fugitive leakage that were difficult to capture. As shown in Figure 1,  
464 the GDP and vehicle population grew by 40% and 24%, respectively, while coal  
465 consumption declined slightly during 2015-2019. Along with stringent emission  
466 reduction actions, the provincial emissions of SO<sub>2</sub>, NO<sub>x</sub> and PM<sub>2.5</sub> were gradually  
467 decoupling from those economical and energy factors, while CO was still strongly  
468 influenced by the change of coal consumption.

469 We present the sectoral contribution to anthropogenic emissions and their interannual  
470 changes in Figure 2 and Figure 3, respectively. Industrial sector was identified as the  
471 major contributor to SO<sub>2</sub>, CO, AVOCs, PM<sub>10</sub>, and PM<sub>2.5</sub> emissions, of which the  
472 contribution accounted averagely for 50%, 62%, 64%, 68%, and 61% during  
473 2015-2019, respectively (Figure 2a, c, d, f and g). The sector was found to drive the  
474 reductions in emissions of SO<sub>2</sub>, NO<sub>x</sub>, CO, PM<sub>10</sub>, PM<sub>2.5</sub> and BC. In particular, the  
475 benefit of emission controls on industrial sector after 2017 was found to clearly  
476 elevate, and to surpass that of power sector for SO<sub>2</sub>, NO<sub>x</sub>, PM<sub>10</sub> and PM<sub>2.5</sub> (Figure 3a,  
477 b, f and g).

478 The power sector, accounting for more than half of provincial coal burning though,  
479 was not the most important contributor to the emissions of any pollutant (Figure 2).  
480 Upgrading the units with advanced APCDs, phasing-out outdated boilers, and  
481 retrofitting for ultra-low emission requirement significantly reduced SO<sub>2</sub>, NO<sub>x</sub>, and  
482 particulate emissions from the power sector (Liu et al., 2015; Zhang et al., 2021b).  
483 With the completion of the ultra-low emission retrofit in 2017, the declines of  
484 emissions for most species slowed down for the power sector (Figure 3). The results  
485 indicated that the potential for further emission abatement from end-of-pipe controls  
486 has been very limited for the sector, unless an energy transition with less coal  
487 consumption is sustainably undertaken in Jiangsu.

488 The transportation sector averagely accounted for 51%, 17%, 14% and 42% of NO<sub>x</sub>,  
489 CO, AVOCs and BC emissions, respectively (Figure 2b, c, d, and h). The growth of  
490 vehicle population resulted in a 38% increase in the annual NO<sub>x</sub> emissions from  
491 transportation from 2015 to 2019, faster than that of any other sector (Figure 3b).  
492 Similarly, a 20% and 25% increase were found for transportation CO and BC

删除的内容: d

494 emissions (Figure 3c and h), respectively. Therefore, the rapid development of  
495 transportation in economically developed Jiangsu has expanded its contribution to air  
496 pollutant emissions for those species, particularly after the emissions from large  
497 power and industrial plants have been effectively curbed. However, the  
498 implementation of China V emission standard (equal to Euro V,  
499 <https://publications.jrc.ec.europa.eu/repository/handle/JRC102115>) for motor vehicles  
500 since 2018 effectively slowed down the growth of transportation NO<sub>x</sub> emissions: The  
501 annual growth rate was estimated to decrease from 12% for 2015-2017 to 5% in  
502 2018-2019. Meanwhile, a downward trend was also found for transportation AVOCs  
503 emissions since 2018 (Figure 3d). Those results show that emission controls for  
504 transportation could be crucial for limiting the key precursors of ozone production  
505 (Geng et al., 2021; Zhang et al., 2019a).

506 The residential sector was the most important source of OC, contributing averagely 68%  
507 to total emissions within 2015-2019 (Figure 2i), and was the second most important  
508 source of PM<sub>10</sub> (18%, Figure 2f) and PM<sub>2.5</sub> (24%, Figure 2g). It dominated the  
509 abatement of OC emissions, attributed to the reduced bulk coal and straw burning  
510 (Figure 3i). The agricultural sector dominated NH<sub>3</sub> emissions (91%, Figure 2e), and  
511 the small decline resulted mainly from the reduced use of nitrogen fertilizer (13%)  
512 from 2015 to 2019 (Figure 3e).

513 It is worth noting that the PM<sub>2.5</sub> and OC emissions decreased faster than BC (Figure  
514 2g-i). As mentioned above, the reduction in primary PM<sub>2.5</sub> resulted mainly from the  
515 improved energy efficiencies and emission controls in industry, and promotion of  
516 clean stoves and replacement of solid fuels with natural gas and electricity in  
517 residential sources. For OC, in particular, the reduced use of household biofuel and  
518 the prohibition of open biomass burning led to considerable emission abatement (18%  
519 from 2015 to 2019). However, the lack of specific APCDs and increasing heavy-duty  
520 diesel vehicles partly offset the benefit of emission controls for other sources,  
521 resulting relatively small reduction in BC emissions (6%). Besides air quality issue,  
522 the slower decline of BC than OC raised the regional climate challenge, as the former  
523 has a warming impact while the latter a cooling one.

### 524 3.1.2 City-level emissions and spatial distribution

525 Figure 4 and Table S5 in the supplement shows the average annual emissions of SO<sub>2</sub>,  
526 NO<sub>x</sub>, AVOCs, NH<sub>3</sub>, and PM<sub>2.5</sub> for the five years by city. In further discussions, we  
527 classified the 13 cities in Jiangsu as the southern cities (Nanjing, Zhenjiang,  
528 Changzhou, Wuxi, and Suzhou), central cities (Yangzhou, Taizhou, and Nantong) and  
529 northern cities (Xuzhou, Suqian, Lianyungang, Huaian, and Yancheng) (their  
530 distributions are shown in Figure S1). Clearly larger emissions of most species were  
531 found in southern Jiangsu cities with more developed industrial economy and  
532 transportation (Figure 4a-e, see the detailed emission data by year in Table S5). The  
533 SO<sub>2</sub> emissions per unit area were calculated as 7.7, 3.3, and 2.4 ton·km<sup>-2</sup> for the  
534 southern, central and northern cities, respectively. The analogous numbers were 23.0,  
535 11.7, and 8.1 ton·km<sup>-2</sup> for NO<sub>x</sub>, 22.5, 13.2, and 8.1 ton·km<sup>-2</sup> for AVOCs, and 7.3, 5.2,  
536 and 2.9 ton·km<sup>-2</sup> for PM<sub>2.5</sub>, respectively. As shown in Figure S3 in the Supplement,  
537 the regions along the Yangtze River are of largest densities of power and industrial  
538 plants. In contrast, higher NH<sub>3</sub> emissions were found for the central and northern  
539 cities with abundant agricultural activities (Figure 4e). Figure S4 in the Supplement  
540 illustrates the spatial distributions of emissions for selected species for 2019, at a  
541 horizontal resolution of 3km. Besides industrial sources, the spatial patterns of NO<sub>x</sub>,  
542 BC, CO and AVOCs were also influenced by the road net, suggesting the role of  
543 heavy traffic on emissions. Particulate matter emissions were mainly distributed in  
544 urban industrial regions, while OC was more found in the broader central and  
545 northern areas, attributed partly to the contribution from residential biofuel use.

546 According to Table S5, faster declines in annual SO<sub>2</sub>, NO<sub>x</sub> and PM<sub>2.5</sub> emissions for  
547 southern cities (59%, 23%, and 24% from 2015 to 2019, respectively) could be found  
548 than for northern cities (53%, 18%, and 8%, respectively). In contrast, AVOCs  
549 emissions were estimated to increase by 10% in southern cities while decrease by 27%  
550 in northern cities. The fractions of southern cities to the total provincial emissions  
551 decreased from 2015 to 2019 except for AVOCs and NH<sub>3</sub>, indicating more benefits of  
552 stringent measures on emission controls for relatively developed regions (Figure 4f).

553 Figure 5 illustrates the changes in the spatial distribution of major pollutant emissions  
554 from 2015 to 2019 in Jiangsu. It can be found that the areas with large emission  
555 reduction for SO<sub>2</sub>, NO<sub>x</sub>, and PM<sub>2.5</sub> were consistent with the locations of super  
556 emitters of corresponding species (Figure 5a-c). Facing bigger challenges in air  
557 quality improvement, the economically developed southern Jiangsu has made more  
558 efforts on the emission controls of large-scale power and industrial enterprises, and  
559 achieved greater emission reduction than the less developed northern Jiangsu.  
560 Different pattern in the spatial variation of emissions was found for AVOCs (Figure  
561 5d). There was a big development of industrial parks for chemical engineering along  
562 the riverside of Yangtze River in the cities of Suzhou, Nantong, and Wuxi in southern  
563 Jiangsu. The elevated solvent use and output of chemical products of those large-scale  
564 enterprises resulted in the growth of AVOCs emissions. In northern Jiangsu, in  
565 contrast, small-scale chemical plants have been gradually closed, and the emissions  
566 were thus effectively reduced. There is a great need for substantial improvement of  
567 emission controls for the key regions and sectors for further abatement of AVOCs  
568 emissions.

### 569 **3.1.3 Enhanced contribution of biogenic sources to total NMVOCs**

570 Table 1 summarizes AVOCs and BVOCs emissions by month and year. Different from  
571 AVOCs that decreased slowly but continuously from 2015 to 2019, a clearly growth  
572 of annual BVOCs emissions was estimated between 2015 and 2017, followed by a  
573 slight reduction till 2019. The peak annual BVOCs emissions reached 213 Gg in 2017.  
574 The interannual variation of BVOCs was mainly associated to that of temperature and  
575 short-wave radiation (Wang et al., 2020b). Influenced by meteorological conditions  
576 and vegetation growing, BVOCs emissions were most abundant in July, less in April  
577 and October and almost zero in January. Within the province, there was a general  
578 increasing gradient from southeast to northwest in BVOCs emissions (Figure S5 in  
579 the Supplement). The rapid development of industrial economy in southern Jiangsu  
580 has led to the expansion of urban centers and less vegetation cover, which limited the

581 BVOCs emissions.  
582 We calculated the ratio of BVOCs to AVOCs emissions by month and year (Table 1).  
583 Dependent on the trends of both BVOCs and AVOCs emissions, the annual ratio  
584 increased from  $11.1 \times 10^{-2}$  in 2015 to  $15.8 \times 10^{-2}$  in 2017, and stayed above  $15 \times 10^{-2}$   
585 afterwards. There is also a clear seasonal difference in the ratio, with the averages for  
586 the five years estimated at  $0 \times 10^{-2}$ ,  $8 \times 10^{-2}$ ,  $52 \times 10^{-2}$ , and  $3 \times 10^{-2}$  for January, April, July  
587 and October, respectively. Since 2016, the ratio of BVOCs to AVOCs emissions  
588 exceeded  $50 \times 10^{-2}$  in July, indicating that the  $O_3$  pollution in summer could be  
589 increasingly influenced by BVOCs. Regarding the spatial pattern, larger ratios were  
590 commonly found in northern Jiangsu, with a modest growth for recent years (Figure  
591 6). Moreover, greater growth of the ratio was found in part of southern Jiangsu where  
592 AVOCs emissions were rapidly declining (e.g., Nanjing and Zhenjiang). The  
593 evolution indicated that biogenic sources became more influential in  $O_3$  production  
594 even for some regions with developed industrial economy, along with controls of  
595 anthropogenic emissions. Due to the relatively high level of ambient  $NO_2$  from  
596 anthropogenic emissions, a broad area of Jiangsu was identified with a mixed or  
597 VOC-limited regime in terms of  $O_3$  formation (Jin and Holloway, 2015), indicating  
598 the impacts of NMVOCs (including BVOCs) on the ambient  $O_3$  concentration. In the  
599 future, the BVOCs emissions may further increase with the elevated temperature,  
600 improved afforestation and vegetation protection, and they will probably play a more  
601 important role on summer  $O_3$  pollution once the controls of AVOCs emissions are  
602 pushed forward (Ren et al., 2017; Gao et al., 2022a).

删除的内容: s

删除的内容: were

## 605 **3.2 The comparisons between different emission inventories**

### 606 **3.2.1 Assessment of emission amounts**

607 We compared our provincial-level emission inventory with previous studies on  
608 emissions in Jiangsu in terms of the total and sectoral emissions through examinations  
609 of activity data, emission factor, removal efficiency and other parameters. The  
610 influence of data and methods on emission estimation was then revealed.

611 Table 2 compares our emission estimates, by year and species, with available global  
612 (EDGAR, Crippa et al., 2020), continental (REAS, Kurokawa et al., 2020), national  
613 (MEIC), and regional emission inventories (Li et al., 2018; Sun et al., 2018; Zhang et  
614 al., 2017b; Simayi et al., 2019; An et al., 2021; Gao et al., 2022b; Yang et al., 2021a),  
615 official emission statistics of Jiangsu Province  
616 (<http://sthjt.jiangsu.gov.cn/col/col83555/index.html>), and an emission estimate with  
617 the “top-down” approach, i.e., constrained by satellite observation and inverse  
618 chemistry transport modelling (Yang et al., 2019). In particular, we stressed the  
619 differences in emissions by sector among our study, MEIC and An et al. (2021) for  
620 2017 as an example (Figure 8).

621 The annual SO<sub>2</sub> emissions in our provincial inventory were close to those in REAS  
622 (2015), MEIC, Yang et al. (2021a), and official statistics for most years, but much  
623 smaller than those reported by EDGAR, Sun et al. (2018) and Li et al. (2018). The  
624 emissions in this work were 32% higher than the MEIC for 2017, with the biggest  
625 difference (62% higher in this work) for power sector (Figure 8). It results mainly  
626 from the discrepancies in the penetration and SO<sub>2</sub> removal efficiency of flue gas  
627 desulfurization (FGD) systems applied in the two emission inventories. For example,  
628 Zhang et al. (2019a) assumed that the penetration rate of FGD in the coal-fired power  
629 sector reached 99.6% in 2017, with the removal efficiency estimated at 95%.  
630 According to our unit-based investigation, the removal efficiencies in the power  
631 sector were typically less than 92%, owing to the aging devices, low flue gas  
632 temperature and other reasons. The main differences between this work and the YRD

633 emission inventory by An et al. (2021) existed in the industrial sector, attributed partly  
634 to insufficient consideration of the comprehensive emission control regulations of  
635 coal-fired boilers in Jiangsu in the past few years in An et al. (2021).

636 The estimates of NO<sub>x</sub> emissions from MEIC, EDGAR and Sun et al. (2018) were  
637 14-38% higher than ours, while the official statistics were much lower than ours,

删除的内容: smaller

638 attributed mainly to the absence of emissions from traffic sources in the statistics. The  
639 major difference between MEIC and our provincial inventory existed in the power  
640 and industrial sector, and the total emissions in the former were 56% larger than the  
641 latter (Figure 8). For example, the emission factors for coal-fired power plants in this  
642 study were derived from CEMS (0.03-2.8 g·kg<sup>-1</sup> coal), much smaller than those from  
643 applied in MEIC and another research (2.88-8.12 g·kg<sup>-1</sup> coal, Zhang et al., 2021b).  
644 Similarly, the smaller emission factors for industrial boilers derived based on on-site  
645 investigations were commonly smaller than previous studies, leading to an estimation  
646 of 45% smaller than MEIC for industrial sector in 2017. Correspondingly, some  
647 modeling and satellite studies suggested that the NO<sub>x</sub> emissions in previous studies  
648 were overestimated partly due to less consideration of improvement in NO<sub>x</sub> control  
649 measures for coal burning sources (Zhao et al., 2018; Sha et al., 2019). Constrained by  
650 satellite observation, the top-down estimation by Yang et al. (2019) was 10% and 22%  
651 smaller than our provincial emission estimation and MEIC for 2016.

652 As mentioned in Section 2.1.2, AVOCs emissions for certain industrial sources in this  
653 study were estimated with a procedure-based approach, which took the removal  
654 efficiencies of different technologies into account (Zhang et al., 2021a). Therefore, the  
655 annual AVOCs emissions in the provincial inventory were commonly much smaller  
656 than others. Without sufficient the local information, for example, Simayi et al. (2019)  
657 applied the national average removal efficiencies of AVOCs in furniture  
658 manufacturing, automotive manufacturing and textile dyeing industries at 18%, 28%,  
659 and 30%, clearly lower than 21%, 42%, and 43% in our inventory, respectively. As a  
660 result, the AVOCs emissions from industrial source in the former were 45% higher  
661 than the latter.

662 NH<sub>3</sub> emissions in the provincial emission inventory were commonly smaller than

664 others. In particular, the estimate was less than half of that by An et al. (2021) for  
665 2017 (Figure 8). The big difference resulted mainly from the methodologies. As  
666 indicated by our previous study (Zhao et al., 2020), the method characterizing  
667 agricultural processes usually provided smaller emission estimates than that using the  
668 constant emission factors. The former detected the emission variation by season and  
669 region, and was more supportive for air quality modeling with better agreement with  
670 ground and satellite observation. Compared with Infrared Atmospheric Sounding  
671 Interferometer (IASI) observation, for example, application of the emission inventory  
672 characterizing agricultural processes in CMAQ reduced the monthly NMEs of vertical  
673 column density of  $\text{NH}_3$  from 44%-84% to 38%-60% in different seasons for the YRD  
674 region (Zhao et al., 2020).

675 For PM emissions, our estimates were larger than MEIC, Gao et al. (2022b), An et al.  
676 (2021) and official emission statistics, but smaller than EDGAR, REAS, and Yang et  
677 al. (2021a). The discrepancies resulted mainly from the inconsistent penetration rates  
678 and removal efficiencies of dust collectors determined at national level and from  
679 on-site surveys at provincial level. Taking cement as an example, all the plants were  
680 assumed to be installed with dust collectors, and the national average removal  
681 efficiency was determined at 99.3% in MEIC (Zhang et al., 2019a), clearly larger than  
682 that in Jiangsu from plant-by-plant surveys (93%). The  $\text{PM}_{10}$  and  $\text{PM}_{2.5}$  emissions  
683 from the industrial sector in this study were 197 and 113 Gg higher than MEIC for  
684 2017 (Figure 8).

### 685 **3.2.2 Assessment of interannual variability**

686 Figure 7 compares the interannual trends of  $\text{SO}_2$  and  $\text{NO}_x$  emissions estimated in this  
687 study with those in available global (EDGAR) and national emission inventories  
688 (MEIC), as well as those of annual averages of ambient concentrations for  
689 corresponding species collected from the state-operating observation sites in Jiangsu.  
690 Different from other inventories, the global emission inventory EDGAR could not  
691 reflect the rapid decline of  $\text{SO}_2$  and  $\text{NO}_x$  emissions of Jiangsu for recent years. It is



692 probably due to the lack of information on the gradually enhanced penetrations and  
693 removal efficiencies of APCDs use in power and industrial sectors in EDGAR.  
694 Therefore, we mainly compared the interannual variability of emissions in our  
695 provincial inventory and MEIC.

696 Both MEIC and our provincial inventory show the continuous declines in SO<sub>2</sub> and  
697 NO<sub>x</sub> emissions for Jiangsu from 2015 to 2019, which could be partly confirmed by  
698 the ground observation. In general, quite similar trends were found for the two  
699 inventories, suggesting similar estimations in the interannual variation of total  
700 emissions at the national and provincial scales. However, there are some discrepancies  
701 between the two. Compared to MEIC, as shown in Figure 7a, a slower decline in SO<sub>2</sub>  
702 emissions between 2015 and 2017 was estimated by our provincial inventory, but a  
703 faster one between 2017 and 2019. In other words, MEIC describes a more optimistic  
704 emission abatement for earlier years. The ultra-low emission retrofit on power sector  
705 started from 2015 in Jiangsu, which was expected to significantly reduce the  
706 emissions of coal-fired plants to the level of gas-fired ones. Through investigations  
707 and examinations of information on APCD operations for individual sources, we  
708 cautiously speculated that the benefit of the retrofit might not be as large as expected  
709 at the initial stage. This could be partly supported by the correspondence between  
710 online monitoring of SO<sub>2</sub> emissions for individual power plants and satellite-derived  
711 SO<sub>2</sub> columns around them when the ultra-low emission retrofit was required (Karplus  
712 et al., 2018). From 2017 to 2019, we were more optimistic on the emission reduction,  
713 attributed partly to larger benefit of emission controls on non-electric industries.  
714 Similar case with less discrepancy could also be found for NO<sub>x</sub> emission (Figure 7b).

删除的内容: greatly

### 715 **3.3 Analysis of driving force of emission change from 2015 to 2019**

716 The actual reductions of annual SO<sub>2</sub>, NO<sub>x</sub>, AVOCs, NH<sub>3</sub>, and PM<sub>2.5</sub> emissions were  
717 estimated at 331, 289, 77, 46, and 80 Gg from 2015 to 2019, respectively in our  
718 provincial emission inventory. We analyzed the emission abatement and its driving  
719 forces for two periods, 2015-2017 and 2017-2019, to represent the different influences

721 of individual measures on emissions for NAPAPCP and TYAPFAP. As shown in  
722 Figure S6 in the Supplement, the actual emission reductions of SO<sub>2</sub> and NH<sub>3</sub> during  
723 2015-2017 (211 and 34 Gg respectively) exceeded those during 2017-2019 (120 and  
724 12 Gg, respectively). As the retrofit of ultra-low emission technologies for the power  
725 sector and the modification of large-scale intensive management of livestock farming  
726 in Jiangsu were basically completed between 2015 and 2017. The reductions of  
727 annual NO<sub>x</sub>, AVOCs, and PM<sub>2.5</sub> emissions during 2017-2019 were much larger (209,  
728 72, and 57 Gg, respectively) than those during 2015-2017 (80, 5, and 23 Gg,  
729 respectively), implying bigger benefits of TYAPFAP on emission controls of those  
730 species.

731 Figure 9 summarizes the effect of individual measures on net emission reduction for  
732 the two periods. There were some common measures for SO<sub>2</sub>, NO<sub>x</sub> and PM<sub>2.5</sub>  
733 emission controls, thus, they were further discussed together below. During  
734 2015-2017, the ultra-low emission retrofit of coal-fired power plants was identified to  
735 be the most important driving factor for the reductions of SO<sub>2</sub> and NO<sub>x</sub> emissions,  
736 responsible for 38% and 43% of the abatement for the two species, respectively. By  
737 the end of 2017, more than 95% of the coal-fired power plants in Jiangsu were  
738 equipped with FGD and selective catalytic/non-catalytic reduction (SCR/SNCR), and  
739 91% of coal-fired power generation capacity met the ultra-low emission standards (35,  
740 50 and 10 mg·m<sup>-3</sup> for SO<sub>2</sub>, NO<sub>x</sub> and PM concentration in the flue gas, respectively;  
741 Zhang et al., 2019a). Through the information cross check and incorporation based on  
742 different emission source databases as mentioned in Section 2.1.3, the average  
743 removal efficiencies of SO<sub>2</sub> and NO<sub>x</sub> in the coal-fired power plants were estimated to  
744 increase from 89% and 50% in 2015 to 94% and 63% in 2017, respectively.

745 The extensive management of coal-fired boilers was the second most important driver  
746 for SO<sub>2</sub> and NO<sub>x</sub> reduction and the most important driver for PM<sub>2.5</sub>, contributing to  
747 24%, 20% and 37% of the emission reductions for corresponding species, respectively.  
748 The main actions included the elimination of 100 MW of coal-fired power generation  
749 capacity and the enhanced penetrations of SO<sub>2</sub> and particulate control devices on large  
750 coal-fired industrial boilers since the improved enforcement of the latest emission

751 standard (GB 13271–2014).

752 The upgradation and renovation of non-electrical industry contributed 18%, 15%, and  
753 28% to the emission reductions for SO<sub>2</sub>, NO<sub>x</sub>, and PM<sub>2.5</sub>, respectively. Till 2017,  
754 more than 80% of steel-sintering machines and cement kilns were equipped with FGD  
755 and SCR/SNCR systems. The average removal efficiency in the steel and cement  
756 production increased from 48% and 43% in 2015 to 60% and 57% in 2017 for SO<sub>2</sub>,  
757 and from 45% and 38% in 2015 to 54% and 40% in 2017 for NO<sub>x</sub>, respectively (as  
758 shown in Figure S7 in the Supplement).

759 Phasing out outdated capacities in key industries including crude steel (8 million tons),  
760 cement (9 million tons), flat glass (3 million weight-boxes), and other  
761 energy-inefficient production capacity contributed 11%, 6%, and 11% to the emission  
762 reductions of corresponding species, respectively. Given their relatively small  
763 proportions to total emissions, the contributions of other emission reduction measures  
764 were less than 10%, such as promoting clean energy, phasing out small and polluting  
765 factories, and the construction of port shore power.

766 The driving forces of emission abatement have been changing for the three species  
767 since implementation of TYAPFAP. The potential for further reduction of SO<sub>2</sub> and  
768 NO<sub>x</sub> emissions were narrowed through the end-of-pipe treatment in the power sector,  
769 and the ultra-emission retrofit on the sector was of very limited influence on the  
770 emissions during 2017-2019. Measures on the non-electric sector brought greater  
771 benefits on emission reduction. Extensive management of coal-fired boilers and  
772 upgradation and renovation of non-electrical industry maintained as the most  
773 important driving factors for the reduction of SO<sub>2</sub>, NO<sub>x</sub>, and PM<sub>2.5</sub> emissions (33%,  
774 20%, and 26% for the former and 28%, 29% and 33% for the latter, respectively).

775 After 2017, small coal boilers ( $\leq 30$  MW) were continuously shut down and remaining  
776 larger ones ( $\geq 60$  MW) were all retrofitted with ultra-low emission technology.  
777 Through the ultra-low emission retrofit, the average removal efficiencies of NO<sub>x</sub> in  
778 the steel and cement production increased from 54% and 40% in 2017 to 70% and 61%  
779 in 2019, respectively.

780 Regarding AVOCs, the emission reduction resulted mainly from the implementation

781 of controls on the key sectors, which accounted for 63% and 34% of the reduced  
782 emissions for 2015-2017 and 2017-2019, respectively. Besides, application of LDAR  
783 was the second most important measure for 2015-2017, with the contribution to  
784 emission reduction reaching 23%. The results also showed that AVOCs emission  
785 reductions from all the concerned measures in 2017-2019 (152Gg) were higher than  
786 those in 2015-2017 (116 Gg). Although more abatement in total AVOCs emissions  
787 was found for 2017-2019 (Figure S6), the contributions of above-mentioned two  
788 measures reduced clearly in the period. Some other measures were identified to be  
789 important drivers of emission reduction, including control on mobile sources (e.g.,  
790 implementation of the China V emission standard for on-road vehicles) and  
791 replacement with low-VOCs paints. In our recent studies, we evaluated the average  
792 removal efficiency of AVOCs in industrial sector was less than 30% (Zhang et al.,  
793 2021a), and organic solvents with low-VOCs content accounted for less than 30% of  
794 total solvent use (Wu et al., 2022). Therefore, there would still be great potential for  
795 further reduction of AVOCs emissions through improvement on the end-of-pipe  
796 emission controls and use of cleaner solvents.

797 In summary, expanding the end-of-pipe treatment (e.g., the ultra-low emission retrofit)  
798 from power to non-electricity industry and phasing out the outdated industrial  
799 capacities have driven the declines of emissions for most species. Along with the  
800 limited potential for current measures, more substantial improvement of energy and  
801 industrial structures could be the option for further emission reduction in the future.

## 802 **3.4 Effectiveness of emission controls on the changing air quality**

### 803 **3.4.1 Simulation of the O<sub>3</sub> and PM<sub>2.5</sub> concentrations**

804 The CMAQ model performance was evaluated with available ground observation.  
805 The observed concentrations of PM<sub>2.5</sub> (hourly) and O<sub>3</sub> (the maximum daily 8-h  
806 average, MDA8) were compared with the simulations using the provincial emission  
807 inventory and MEIC for the selected four months for 2015-2019, as summarized in  
808 Table S6 and Table S7 in the Supplement. Overall, the simulation with the provincial

809 inventory shows acceptable agreement with the observations, with the annual means  
810 of NMB and NME ranging -21% – 2% and 43% –52% for PM<sub>2.5</sub>, and -26% – -14%  
811 and 30% – 41% for O<sub>3</sub>. The analogous numbers for MEIC were -23% – -5% and 47%  
812 – 53% for PM<sub>2.5</sub>, and -26% – -6% and 33% – 46% for O<sub>3</sub>, respectively. Most of the  
813 NMB and NME were within the proposed criteria ( $-30\% \leq \text{NMB} \leq 30\%$  and  $\text{NME} \leq 50\%$ ,  
814 Emery et al., 2017). Better performance was achieved using the provincial inventory,  
815 implying the benefit of applying refined emission data on high-resolution air quality  
816 simulation.

817 Besides O<sub>3</sub> and PM<sub>2.5</sub>, better model performances were also found for SO<sub>2</sub> and NO<sub>2</sub>  
818 with the provincial emission inventory than MEIC, as shown [in](#) Table S8 in the  
819 Supplement. For 2017, the monthly NMB and NME ranged -38% – -24% and 43% –  
820 53% for SO<sub>2</sub>, and 22% – 40% and 38% – 61% for NO<sub>2</sub>. The analogous numbers for  
821 MEIC were 35% – 68% and 84% – 114% for SO<sub>2</sub>, and 50% – 133% and 65% – 138%  
822 for NO<sub>2</sub>, respectively (unpublished data provided by MEIC development team,  
823 Tsinghua University).

824 Figure 10 compares the observed and simulated (with the provincial inventory)  
825 interannual trends in PM<sub>2.5</sub> and MDA8 O<sub>3</sub> concentrations from 2015 to 2019 (see the  
826 simulated spatiotemporal evolution in Figures S8 and S9 in the Supplement).  
827 Satisfying correlations between observed and simulated concentrations were found for  
828 both PM<sub>2.5</sub> and MDA8 O<sub>3</sub>, with the squares of correlation coefficients ( $R^2$ ) estimated  
829 at 0.81 and 0.86 within the research period, respectively. The good agreement  
830 suggests the simulation with high-resolution emission inventory was able to well  
831 capture the interannual changes in air quality at the provincial scale.

832 Both observation and simulation indicated a declining trend of PM<sub>2.5</sub> concentrations,  
833 with the annual decreasing rates estimated at -5.4 and -4.2  $\mu\text{g}\cdot\text{m}^{-3}\cdot\text{yr}^{-1}$ , respectively  
834 (Figure 10a). The decline reflected the benefit of improved implementation of  
835 emission control actions as well as the influence of meteorological condition change.  
836 In general, higher concentrations were found in winter and lower in summer. A  
837 rebound in PM<sub>2.5</sub> level was notably found in winter after 2017, attributed possibly to

838 the unfavorable meteorological conditions that were more likely to exacerbate air  
839 pollution (e.g., the reduced wind speed as shown in Table S2) for recent years. In  
840 contrast to PM<sub>2.5</sub>, MDA8 O<sub>3</sub> was clearly elevated from 2015 to 2019, with the annual  
841 growth rates estimated at 4.6 and 7.3 μg·m<sup>-3</sup>·yr<sup>-1</sup>, by observation and simulation  
842 (Figure 10b). Higher concentrations were found in spring and summer and lower in  
843 autumn and winter. Besides the impact of emission change, the O<sub>3</sub> concentrations can  
844 be greatly influenced by the varying meteorological factors such as the decreased  
845 relative humidity and wind speed for recent years in YRD region (Gao et al., 2021;  
846 Dang et al., 2021). In addition, the recent declining PM<sub>2.5</sub> concentration in eastern  
847 China reduced the heterogeneous absorption of hydroperoxyl radicals (HO<sub>2</sub>) by  
848 aerosols and thereby enhanced O<sub>3</sub> concentration (Li et al., 2019). If such aerosol  
849 effect was considered in CMAQ modeling, the increasing rate of annual O<sub>3</sub>  
850 concentration would possibly be further overestimated. The complex impacts of  
851 various factors on air quality triggered the separation of emission and meteorological  
852 contributions to the changing PM<sub>2.5</sub> and O<sub>3</sub> levels in Section 3.4.2.

853 The common underestimation of O<sub>3</sub> should be stressed, partly resulting from the bias  
854 in the estimation of precursor emissions. In this study, the enhanced penetrations  
855 and/or removal efficiencies of NO<sub>x</sub> control devices might not be fully considered in  
856 the emission inventory development, in particular for the non-electric industry,  
857 leading to possible overestimation of NO<sub>x</sub> emissions. Moreover, underestimation of  
858 AVOCs emissions could exist, due to incomplete counting of emission sources,  
859 particularly for the uncontrolled fugitive leakage. As most of Jiangsu was identified as  
860 a VOC-limited region for O<sub>3</sub> formation (Wang et al., 2020b; Yang et al., 2021b), the  
861 overestimation of NO<sub>x</sub> and underestimation of AVOCs could result in underestimation  
862 in O<sub>3</sub> concentration with air quality modeling. Compared to MEIC, the improved  
863 provincial emission inventory partly corrected the overestimation of NO<sub>x</sub> emissions  
864 and NO<sub>2</sub> concentrations (Table S8), and helped reduce the bias of O<sub>3</sub> concentration  
865 simulation. Furthermore, a larger underestimation in O<sub>3</sub> was revealed before 2017  
866 (Figure 8b), attributed partly to less data support on the emission sources and thereby  
867 less reliability in the emission inventory, compared with more recent years.

删除的内容: involved

删除的内容: complicated

### 870 3.4.2 Anthropogenic and meteorological contribution to O<sub>3</sub> and PM<sub>2.5</sub> variation

871 As shown in Figure 11, in the baseline simulation that accounted for the interannual  
872 changes of both anthropogenic emissions and meteorology, the provincial-level PM<sub>2.5</sub>  
873 concentration (geographical mean) was calculated to decrease by 4.1 μg·m<sup>-3</sup> in  
874 2015-2017 and 1.7 μg·m<sup>-3</sup> in 2017-2019, and MDA8 O<sub>3</sub> increase by 17.0 μg·m<sup>-3</sup> in  
875 2015-2017 and 3.2 μg·m<sup>-3</sup> in 2017-2019. Smaller variations were found for more

876 recent years for both species. With VEMIS and VMET, the contributions of the two  
877 factors were identified and discussed in the following. It should be noted that the air  
878 quality changes in baseline did not equal to the aggregated contributions in VEMSI  
879 and VMET due to non-linearity effect of the chemistry transport modeling, and the  
880 main goal of the analysis was to compare the relative contributions of the two factors.

881 As shown in Figure 11a, similar patterns of driving factor contributions to PM<sub>2.5</sub> were  
882 found during 2015-2017 and 2017-2019. While meteorological conditions  
883 consistently promoted the formation of PM<sub>2.5</sub>, the continuous abatement of  
884 anthropogenic emissions completely offset the adverse meteorological effects and  
885 contributed to the declines in PM<sub>2.5</sub> concentrations. Although less reduction in PM<sub>2.5</sub>  
886 concentration was found for 2017-2019 due mainly to the worsened meteorology,  
887 emission abatement was estimated to play a greater role on reducing PM<sub>2.5</sub>  
888 concentration (5.5 μg·m<sup>-3</sup> in VEMIS) compared to 2015-2017 (4.3 μg·m<sup>-3</sup>), implying  
889 the higher effectiveness of recent emission control actions on PM<sub>2.5</sub> pollution  
890 alleviation.

891 The O<sub>3</sub> case is different (Figure 11b). Both the changing emissions and meteorology  
892 favored MDA8 O<sub>3</sub> increase for 2015-2017, consistent with previous studies (Wang et  
893 al., 2019; Dang et al., 2021). The contribution of meteorology was estimated at 11.9  
894 μg·m<sup>-3</sup> (VMET), larger than that of emissions at 4.9 μg·m<sup>-3</sup> (VEMIS). As shown in  
895 Figure S6, the abatement of annual NO<sub>x</sub> emissions in Jiangsu was estimated at 104  
896 Gg, while very limited reduction was achieved in AVOCs emissions. Declining NO<sub>x</sub>  
897 emissions thus elevated O<sub>3</sub> formation under the VOC-limited conditions particularly  
898 in urban areas in Jiangsu.

删除的内容: As shown in Figure 11, the provincial-level PM<sub>2.5</sub> concentration (geographical mean) was simulated to decrease by 4.1 μg·m<sup>-3</sup> in 2015-2017 and 1.7 μg·m<sup>-3</sup> in 2017-2019, and MDA8 O<sub>3</sub> increase by 17.0 μg·m<sup>-3</sup> in 2015-2017 and 3.2 μg·m<sup>-3</sup> in 2017-2019, in the baseline that contained the interannual changes of both anthropogenic emissions and meteorology.

910 During 2017-2019, the meteorological condition played a more important role on the  
911 O<sub>3</sub> growth (14.3 μg·m<sup>-3</sup>), attributed mainly to the decreased relative humidity and  
912 wind speed for recent years (Table S2). In contrast, the changing emissions were  
913 estimated to restrain the O<sub>3</sub> growth by 3.1 μg·m<sup>-3</sup>, implying the effectiveness of  
914 continuous emission controls on O<sub>3</sub> pollution alleviation. As shown in Figure S6, a  
915 much larger reduction in AVOCs emissions was achieved in Jiangsu during  
916 2017-2019 compared to 2015-2017, and the greater NO<sub>x</sub> emission reduction might  
917 have led to the shift from VOC-limited to the transitional regime across the province  
918 (Wang et al., 2021b). The emission controls thus helped limit the total O<sub>3</sub> production.  
919 Although the reduction in precursor emissions was not able to fully offset the effect of  
920 adverse meteorology condition, its encouraging effectiveness demonstrated the  
921 validity of current emission control measures, and actual O<sub>3</sub> decline can be expected  
922 with more stringent control actions to overcome the influence of meteorological  
923 variation.

#### 924 **4. Conclusion remarks**

925 In this study, we developed a high-resolution emission inventory of nine air pollutants  
926 for Jiangsu 2015-2019, by integrating the improvements in methodology for different  
927 sectors and incorporating the best available facility-level information and real-world  
928 emission measurements. We evaluated this provincial-level emission inventory  
929 through comparison with other studies at different spatial scales and air quality  
930 modeling. We further linked the emission changes to various emission control  
931 measures, and evaluated the effectiveness of pollution control efforts on the emission  
932 reduction and air quality improvement.

933 | Our study indicated that the emission controls indeed played an important role in  
934 prevention and alleviation of air pollution. Through a series of remarkable actions in  
935 NAPAPCP and TYAPFAP, the annual emissions in Jiangsu declined to varying  
936 degrees for different species from 2015 to 2019, with the largest relative reduction at  
937 53% for SO<sub>2</sub> and smallest at 6% for AVOCs. Regarding different periods, larger

删除的内容: on



939 abatement of SO<sub>2</sub> emissions was found between 2015 and 2017 but more substantial  
940 reductions of NO<sub>x</sub>, AVOCs and primary PM<sub>2.5</sub> between 2017 and 2019. Our estimates  
941 in SO<sub>2</sub>, AVOCs and NH<sub>3</sub> emissions were mostly smaller than or close to other studies,  
942 while those for NO<sub>x</sub> and primary PM<sub>2.5</sub> were less conclusive. The main reasons for  
943 the discrepancies between studies included the modified methodologies used in this  
944 work (e.g., the procedure-based approach for AVOCs and the agricultural process  
945 characterization for NH<sub>3</sub>) and the varied depths of details on emission source  
946 investigation (e.g., the penetrations and removal efficiencies of APCD). Air quality  
947 modeling confirmed the benefit of refined emission data on predicting the ambient  
948 levels of PM<sub>2.5</sub> and O<sub>3</sub>, as well as capturing their interannual variations.

949 For 2015-2017 within NAPAPCP, the ultra-low emission retrofit on power sector was  
950 most effective on SO<sub>2</sub> and NO<sub>x</sub> emission reduction, but the expansion of emission  
951 controls to non-electricity sectors, including coal-fired boilers and key industries  
952 would be more important for 2017-2019. AVOCs control was still in its initial stage,  
953 and the measures on key industrial sectors and transportation were demonstrated to be  
954 effective. Along with the gradually reduced potential for emission reduction through  
955 end-of-pipe treatment, adjustment of energy and industrial structures should be the  
956 future path for Jiangsu as well as other regions with developed industrial economy.  
957 Air quality modeling suggested worsened meteorological conditions from 2015 to  
958 2019 in terms of PM<sub>2.5</sub> and O<sub>3</sub> pollution alleviation. The continuous actions on  
959 emission reduction, however, have been taking effect on reducing PM<sub>2.5</sub> concentration  
960 and restraining the growth of MDA8 O<sub>3</sub> level.

961 The analysis justified the big efforts and investments by the local government for air  
962 pollution controls, and demonstrated how the investigations of detailed underlying  
963 data could help improve the precision, integrity and continuity of emission inventories.

964 | Such demonstrations were more applicable at regional scale (smaller countries and  
965 territories) instead of national scale due to the huge cost and data gap for the latter.  
966 Furthermore, the work showed how the refined emission data could efficiently  
967 support the high-resolution air quality modeling, and highlighted the varying and  
968 complex responses of air quality to different emission control efforts. Therefore, the

删除的内容: , was

970 study could shed light for other highly polluted regions in China and worldwide, with  
971 diverse stages of regional economical development and air pollution controls.  
972 Limitations remain in the current study. Attributed to insufficient data support, there  
973 was little improvement on emission estimation for some sources compared to previous  
974 studies, e.g., on-road transportation and residential sector. Those sources may play an  
975 increasingly important role on emissions and air quality along with stringent controls  
976 on power and industrial sectors, and thus need to be better stressed in the future. The  
977 temporal profiles of emissions for most source categories were not improved due to  
978 the difficulty in capturing the real-time variation of activity for individual emitters  
979 (e.g., the operation and energy consumption of industrial plant). It could be a reason  
980 for the bias in air quality modeling. Given the limited access on emission source  
981 information, moreover, the emission data for nearby regions around Jiangsu were not  
982 refined in this work. Such limitation might lead to some bias in analyzing the  
983 effectiveness of emission controls on air quality, as regional transport could account  
984 for a considerable fraction of PM<sub>2.5</sub> and O<sub>3</sub> concentrations. Should better regional  
985 emission data get available, more analysis needs to be conducted to separate the  
986 effectiveness of local emission controls and efforts from nearby regions. Due to huge  
987 computational tasks through air quality modeling, the individual emission control  
988 measures were not directly linked to the ambient concentration, and their  
989 effectiveness on air quality improvement cannot be obtained in details. Advanced  
990 numerical tools, e.g., the adjoint modeling, are recommended for further in-depth  
991 analysis.

删除的内容: finally,

## 992 **Data availability**

993 The gridded emission data for Jiangsu Province 2015-2019 can be downloaded at  
994 <http://www.airqualitynju.com/En/Data/List/Datadownload>

## 995 **Author contributions**

996 CGu developed the methodology, conducted the research and wrote the draft. YZhao

998 and LZhang developed the strategy and designed the research, and YZhao revised the  
999 manuscript. ZXu provided the support of air quality modeling. YWang, ZWang and  
1000 HWang provided the support of emission data processing. SXia, LLi, and QZhao  
1001 provided the support of emission data.

## 1002 **Competing interests**

1003 The authors declare that they have no conflict of interest.

## 1004 **Acknowledgments**

1005 This work received support from the Natural Science Foundation of China  
1006 (42177080), the Key Research and Development Programme of Jiangsu Province  
1007 (BE2022838), and Jiangsu Provincial Fund on PM<sub>2.5</sub> and O<sub>3</sub> Pollution Mitigation (No.  
1008 2019023). We appreciate Qiang Zhang, Guannan Geng, and Nana Wu from Tsinghua  
1009 University (the MEIC team) for national emission data and evaluation.

## 1010 **References**

- 1011 An, J., Huang, Y., Huang, C., Wang, X., Yan, R., Wang, Q., Wang, H., Jing, S., Zhang,  
1012 Y., Liu, Y., Chen, Y., Xu, C., Qiao, L., Zhou, M., Zhu, S., Hu, Q., Lu, J., and  
1013 Chen, C.: Emission inventory of air pollutants and chemical speciation for  
1014 specific anthropogenic sources based on local measurements in the Yangtze  
1015 River Delta region, China, *Atmos. Chem. Phys.*, 21, 2003–2025,  
1016 <https://doi.org/10.5194/acp-21-2003-2021>, 2021.
- 1017 Crippa, M., Solazzo, E., Huang G., Guizzardi D., Koffi E., Muntean M., Schieberle C.,  
1018 Friedrich R.: High resolution temporal profiles in the Emissions Database for  
1019 Global Atmospheric Research, *Sci. Data*, 7, 121,  
1020 <https://doi.org/10.1038/s41597-020-0462-2>, 2020.
- 1021 Dang, R., Liao, H., and Fu, Y.: Quantifying the anthropogenic and meteorological  
1022 influences on summertime surface ozone in China over 2012–2017, *Sci. Total*

1023 Environ., 754, 142394, <https://doi.org/10.1016/j.scitotenv.2020.142394>, 2021.

1024 Emery, C., Liu, Z., Russell, A. G., Odman, M. T., Yarwood, G., and Kumar, N.:  
1025 Recommendations on statistics and benchmarks to assess photochemical model  
1026 performance, *J. Air Waste Manag. Assoc.*, 67, 582-598,  
1027 10.1080/10962247.2016.1265027, 2017.

1028 Gao, D., Xie, M., Liu, J., Wang, T., Ma, C., Bai, H., Chen, X., Li, M., Zhuang, B., and  
1029 Li, S.: Ozone variability induced by synoptic weather patterns in warm seasons  
1030 of 2014–2018 over the Yangtze River Delta region, China, *Atmos. Chem. Phys.*,  
1031 21, 5847–5864, <https://doi.org/10.5194/acp-21-5847-2021>, 2021.

1032 Gao, Y., Ma, M., Yan, F., Su, H., Wang, S., Liao, H., Zhao, B., Wang, X., Sun, Y.,  
1033 Hopkins, J. R., Chen, Q., Fu, P., Lewis, A. C., Qiu, Q., Yao, X., and Gao, H.:  
1034 Impacts of biogenic emissions from urban landscapes on summer ozone and  
1035 secondary organic aerosol formation in megacities, *Sci. Total Environ.*, 814,  
1036 152654, <https://doi.org/10.1016/j.scitotenv.2021.152654>, 2022a.

1037 Gao, Y., Zhang, L., Huang, A., Kou, W., Bo, X., Cai, B., and Qu, J.: Unveiling the  
1038 spatial and sectoral characteristics of a high-resolution emission inventory of  
1039 CO<sub>2</sub> and air pollutants in China, *Sci. Total Environ.*, 847, 157623,  
1040 <https://doi.org/10.1016/j.scitotenv.2022.157623>, 2022b.

1041 Geng, G., Zheng, Y., Zhang, Q., Xue, T., Zhao, H., Tong, D., Zheng, B., Li, M., Liu, F.,  
1042 Hong, C., He, K., and Davis, S. J.: Drivers of PM<sub>2.5</sub> air pollution deaths in China  
1043 2002–2017, *Nat. Geosci.*, 14, 645-650, 10.1038/s41561-021-00792-3, 2021.

1044 He K., Zhang Q., Wang S.: Technical manual for the preparation of urban air pollution  
1045 Source emission inventory, China Statistics Press, Beijing, 2018 (in Chinese).

1046 Hsu, C., Chiang, H., Shie, R., Ku, C., Lin, T., Chen, M., Chen, N., and Chen, Y.:  
1047 Ambient VOCs in residential areas near a large-scale petrochemical complex:  
1048 Spatiotemporal variation, source apportionment and health risk, *Environ. Pollut.*,  
1049 240, 95-104, <https://doi.org/10.1016/j.envpol.2018.04.076>, 2018.

1050 Huang, Y., Shen, H., Chen, H., Wang, R., Zhang, Y., Su, S., Chen, Y., Lin, N., Zhuo,  
1051 S., Zhong, Q., Wang, X., Liu, J., Li, B., Liu, W., and Tao, S.: Quantification of  
1052 Global Primary Emissions of PM<sub>2.5</sub>, PM<sub>10</sub>, and TSP from Combustion and

1053 Industrial Process Sources, *Environ. Sci. Technol.*, 48, 13834-13843,  
1054 10.1021/es503696k, 2014.

1055 Huang, Z., Zhong, Z., Sha, Q., Xu, Y., Zhang, Z., Wu, L., Wang, Y., Zhang, L., Cui, X.,  
1056 Tang, M., Shi, B., Zheng, C., Li, Z., Hu, M., Bi, L., Zheng, J., and Yan, M.: An  
1057 updated model-ready emission inventory for Guangdong Province by  
1058 incorporating big data and mapping onto multiple chemical mechanisms, *Sci.*  
1059 *Total Environ.*, 769, 144535, <https://doi.org/10.1016/j.scitotenv.2020.144535>,  
1060 2021.

1061 Hoesly, R. M., Smith, S. J., Feng, L., Klimont, Z., Janssens-Maenhout, G., Pitkanen,  
1062 T., Seibert, J. J., Vu, L., Andres, R.J., Bolt, R. M., Bond, T. C., Dawidowski, L.,  
1063 Kholod, N., Kurokawa, J.-I., Li, M., Liu, L., Lu, Z., Moura, M. C. P., O'Rourke,  
1064 P. R., and Zhang, Q.: Historical (1750–2014) anthropogenic emissions of reactive  
1065 gases and aerosols from the Community Emissions Data System (CEDS), *Geosci.*  
1066 *Model Dev.*, 11, 369–408, <https://doi.org/10.5194/gmd-11-369-2018>, 2018.

1067 Jin, X. and Holloway, T.: Spatial and temporal variability of ozone sensitivity over  
1068 China observed from the Ozone Monitoring Instrument, *J. Geophys. Res.*, 120,  
1069 7229-7246, 10.1002/2015JD023250, 2015.

1070 Karplus, V. J., Zhang, S., and Almond, D.: Quantifying coal power plant responses to  
1071 tighter SO<sub>2</sub> emissions standards in China, *Proc. Natl. Acad. Sci.*, 115, 7004-7009,  
1072 doi:10.1073/pnas.1800605115, 2018.

1073 Ke, J., Li, S., and Zhao, D.: The application of leak detection and repair program in  
1074 VOCs control in China's petroleum refineries, *J. Air Waste Manag. Assoc.*, 70,  
1075 862-875, 10.1080/10962247.2020.1772407, 2020.

1076 Klimont, Z., Smith, S. J., and Cofala, J.: The last decade of global anthropogenic sulfur  
1077 dioxide: 2000–2011 emissions, *Environ. Res. Lett.*, 8, 014003,  
1078 <https://doi.org/10.1088/1748-9326/8/1/014003>, 2013.

1079 Kurokawa, J. and Ohara, T.: Long-term historical trends in air pollutant emissions in  
1080 Asia: Regional Emission inventory in ASia (REAS) version 3, *Atmos. Chem.*  
1081 *Phys.*, 20, 12761–12793, <https://doi.org/10.5194/acp-20-12761-2020>, 2020.

1082 Li, K., Jacob, D. J., Liao, H., Shen, L., Zhang, Q., and Bates, K. H.: Anthropogenic

1083 drivers of 2013-2017 trends in summer surface ozone in China, *Proc. Natl. Acad.*  
1084 *Sci.*, 116, 422-427, doi:10.1073/pnas.1812168116, 2019.

1085 Li, L., An, J. Y., Zhou, M., Qiao, L. P., Zhu, S. H., Yan, R. S., Ooi, C. G., Wang, H. L.,  
1086 Huang, C., Huang, L., Tao, S. K., Yu, J. Z., Chan, A., Wang, Y. J., Feng, J. L.,  
1087 and Chen, C. H.: An integrated source apportionment methodology and its  
1088 application over the Yangtze River Delta region, China, *Environ. Sci. Technol.*,  
1089 52, 14216–14227, 10.1021/acs.est.8b01211, 2018.

1090 Li, M., Zhang, Q., Streets, D. G., He, K. B., Cheng, Y. F., Emmons, L. K., Huo, H.,  
1091 Kang, S. C., Lu, Z., Shao, M., Su, H., Yu, X., and Zhang, Y.: Mapping Asian  
1092 anthropogenic emissions of non-methane volatile organic compounds to multiple  
1093 chemical mechanisms, *Atmos. Chem. Phys.*, 14, 5617–5638,  
1094 <https://doi.org/10.5194/acp-14-5617-2014>, 2014.

1095 Liu, F., Zhang, Q., Tong, D., Zheng, B., Li, M., Huo, H., and He, K. B.:  
1096 High-resolution inventory of technologies, activities, and emissions of coal-fired  
1097 power plants in China from 1990 to 2010, *Atmos. Chem. Phys.*, 15, 13299–  
1098 13317, <https://doi.org/10.5194/acp-15-13299-2015>, 2015.

1099 Liu, Y., Han, F., Liu, W., Cui, X., Luan, X., and Cui, Z.: Process-based volatile  
1100 organic compound emission inventory establishment method for the petroleum  
1101 refining industry, *J. Clean. Prod.*, 263, 10.1016/j.jclepro.2020.121609, 2020.

1102 Liu, M., Shang, F., Lu, X., Huang, X., Song, Y., Liu, B., Zhang, Q., Liu, X., Cao, J.,  
1103 Xu, T., Wang, T., Xu, Z., Xu, W., Liao, W., Kang, L., Cai, X., Zhang, H., Dai, Y.,  
1104 and Zhu, T.: Unexpected response of nitrogen deposition to nitrogen oxide  
1105 controls and implications for land carbon sink, *Nat. Commun.*, 13, 3126,  
1106 10.1038/s41467-022-30854-y, 2022.

1107 Miyazaki, K., Eskes, H., Sudo, K., Folkert Boersma, K., Bowman, K., and Kanaya, Y.:  
1108 Decadal changes in global surface NO<sub>x</sub> emissions from multi-constituent  
1109 satellite data assimilation, *Atmos. Chem. Phys.*, 17, 807-837,  
1110 10.5194/acp-17-807-2017, 2017.

1111 Mo, Z., Shao, M., and Lu, S.: Compilation of a source profile database for  
1112 hydrocarbon and OVOC emissions in China, *Atmos. Environ.*, 143, 209-217,

1113 <https://doi.org/10.1016/j.atmosenv.2016.08.025>, 2016.

1114 Mo, Z., Lu, S., and Shao, M.: Volatile organic compound (VOC) emissions and health  
1115 risk assessment in paint and coatings industry in the Yangtze River Delta, China,  
1116 *Environ. Pollut.*, 269, 115740, <https://doi.org/10.1016/j.envpol.2020.115740>,  
1117 2021.

1118 National Bureau of Statistics of China: Statistical Yearbook of China, China Statistics  
1119 Press, Beijing, 2016-2021 (in Chinese).

1120 Ren, Y., Qu, Z., Du, Y., Xu, R., Ma, D., Yang, G., Shi, Y., Fan, X., Tani, A., Guo, P.,  
1121 Ge, Y., and Chang, J.: Air quality and health effects of biogenic volatile organic  
1122 compounds emissions from urban green spaces and the mitigation strategies,  
1123 *Environ. Pollut.*, 230, 849-861, <https://doi.org/10.1016/j.envpol.2017.06.049>,  
1124 2017.

1125 Sha, T., Ma, X. Y., Jia, H. L., van der A, R. J., Ding, J. Y., Zhang, Y. L., and Chang, Y.  
1126 H.: Exploring the influence of two inventories on simulated air pollutants during  
1127 winter over the Yangtze River Delta, *Atmos. Environ.*, 206, 170–182,  
1128 <https://doi.org/10.1016/j.atmosenv.2019.03.006>, 2019.

1129 Shen, Y., Wu, Y., Chen, G., Van Grinsven, H. J. M., Wang, X., Gu, B., and Lou, X.:  
1130 Non-linear increase of respiratory diseases and their costs under severe air  
1131 pollution, *Environ. Pollut.*, 224, 631-637, [10.1016/j.envpol.2017.02.047](https://doi.org/10.1016/j.envpol.2017.02.047), 2017.

1132 Simayi, M., Hao, Y. F., Li, J., Wu, R. R., Shi, Y. Q., Xi, Z. Y., Zhou, Y., and Xie, S. D.:  
1133 Establishment of county-level emission inventory for industrial NMVOCs in  
1134 China and spatial-temporal characteristics for 2010–2016, *Atmos. Environ.*, 211,  
1135 194–203, <https://doi.org/10.1016/j.atmosenv.2019.04.064>, 2019.

1136 State Council of the People’s Republic of China. The air pollution prevention and  
1137 control national action plan.  
1138 [http://www.gov.cn/zwggk/2013-09/12/content\\_2486773.htm](http://www.gov.cn/zwggk/2013-09/12/content_2486773.htm).

1139 State Council of the People’s Republic of China. Three-year Action Plan for  
1140 Protecting Blue Sky. Central People's Government of the People's Republic of  
1141 China (2018).  
1142 [http://www.gov.cn/zhengce/content/2018-07/03/content\\_5303158.htm](http://www.gov.cn/zhengce/content/2018-07/03/content_5303158.htm).

1143 Sun, X. W., Cheng, S. Y., Lang, J. L., Ren, Z. H., and Sun, C.: Development of  
1144 emissions inventory and identification of sources for priority control in the  
1145 middle reaches of Yangtze River Urban Agglomerations, *Sci. Total Environ.*, 625,  
1146 155–167, [10.1016/j.scitotenv.2017.12.103](https://doi.org/10.1016/j.scitotenv.2017.12.103), 2018.

1147 Wang, J. D., Zhao, B., Wang, S. X., Yang, F. M., Xing, J., Morawska, L., Ding, A. J.,  
1148 Kulmala, M., Kerminen, V., Kujansuu, J., Wang, Z. F., Ding, D., Zhang, X. Y.,  
1149 Wang, H. B., Tian, M., Petäjä, T., Jiang, J. K., and Hao, J. M.: Particulate matter  
1150 pollution over China and the effects of control policies, *Sci. Total Environ.*, 584–  
1151 585, 426–447, <https://doi.org/10.1016/j.scitotenv.2017.01.027>, 2017.

1152 Wang, N., Xu, J., Pei, C., Tang, R., Zhou, D., Chen, Y., Li, M., Deng, X., Deng, T.,  
1153 Huang, X., and Ding, A.: Air quality during COVID-19 lockdown in the Yangtze  
1154 River Delta and the Pearl River Delta: Two different responsive mechanisms to  
1155 emission reductions in China, *Environ. Sci. Technol.*, 55, 5721–5730,  
1156 [10.1021/acs.est.0c08383](https://doi.org/10.1021/acs.est.0c08383), 2021a.

1157 Wang, P., Guo, H., Hu, J., Kota, S. H., Ying, Q., and Zhang, H.: Responses of PM<sub>2.5</sub>  
1158 and O<sub>3</sub> concentrations to changes of meteorology and emissions in China, *Sci.*  
1159 *Total Environ.*, 662, 297–306, [10.1016/j.scitotenv.2019.01.227](https://doi.org/10.1016/j.scitotenv.2019.01.227), 2019.

1160 Wang, R., Yuan, Z., Zheng, J., Li, C., Huang, Z., Li, W., Xie, Y., Wang, Y., Yu, K., and  
1161 Duan, L.: Characterization of VOC emissions from construction machinery and  
1162 river ships in the Pearl River Delta of China, *J. Environ. Sci., (China)*, 96,  
1163 138–150, [10.1016/j.jes.2020.03.013](https://doi.org/10.1016/j.jes.2020.03.013), 2020a.

1164 Wang, W., van der A, R., Ding, J., van Weele, M., and Cheng, T.: Spatial and temporal  
1165 changes of the ozone sensitivity in China based on satellite and ground-based  
1166 observations, *Atmos. Chem. Phys.*, 21, 7253–7269,  
1167 <https://doi.org/10.5194/acp-21-7253-2021>, 2021b.

1168 Wang, Y., Zhao, Y., Zhang, L., Zhang, J., and Liu, Y.: Modified regional biogenic  
1169 VOC emissions with actual ozone stress and integrated land cover information: A  
1170 case study in Yangtze River Delta, China, *Sci. Total Environ.*, 727, 138703,  
1171 <https://doi.org/10.1016/j.scitotenv.2020.138703>, 2020b.

1172 Wiedinmyer, C., Yokelson, R. J., and Gullett, B. K.: Global Emissions of Trace Gases,



1173 Particulate Matter, and Hazardous Air Pollutants from Open Burning of  
1174 Domestic Waste, *Environ. Sci. Technol.*, 48, 9523-9530, 10.1021/es502250z,  
1175 2014.

1176 Wu, R., Zhao, Y., Xia, S., Hu, W., Xie, F., Zhang, Y., Sun, J., Yu, H., An, J., and Wang,  
1177 Y.: Reconciling the bottom-up methodology and ground measurement constraints  
1178 to improve the city-scale NMVOCs emission inventory: A case study of Nanjing,  
1179 China, *Sci. Total Environ.*, 812, 152447, 10.1016/j.scitotenv.2021.152447, 2022.

1180 Yang, Y., Zhao, Y., Zhang, L., and Lu, Y.: Evaluating the methods and influencing  
1181 factors of satellite-derived estimates of NO<sub>x</sub> emissions at regional scale: A case  
1182 study for Yangtze River Delta, China, *Atmos. Environ.*, 219, 117051,  
1183 <https://doi.org/10.1016/j.atmosenv.2019.117051>, 2019.

1184 Yang, J., Zhao, Y., Cao, J., and Nielsen, C. P.: Co-benefits of carbon and pollution  
1185 control policies on air quality and health till 2030 in China, *Environ. Int.*, 152,  
1186 106482, <https://doi.org/10.1016/j.envint.2021.106482>, 2021a.

1187 Yang, Y., Zhao, Y., Zhang, L., Zhang, J., Huang, X., Zhao, X., Zhang, Y., Xi, M., and  
1188 Lu, Y.: Improvement of the satellite-derived NO<sub>x</sub> emissions on air quality  
1189 modeling and its effect on ozone and secondary inorganic aerosol formation in  
1190 the Yangtze River Delta, China, *Atmos. Chem. Phys.*, 21, 1191–1209,  
1191 <https://doi.org/10.5194/acp-21-1191-2021>, 2021b.

1192 Yen, C. and Horng, J.: Volatile organic compounds (VOCs) emission characteristics  
1193 and control strategies for a petrochemical industrial area in middle Taiwan, *J.*  
1194 *Environ. Health, Part A*, 44, 1424-1429, 10.1080/10934520903217393, 2009.

1195 Zhang, B., Wang, S., Wang, D., Wang, Q., Yang, X., and Tong, R.: Air quality changes  
1196 in China 2013–2020: Effectiveness of clean coal technology policies, *J. Clean.*  
1197 *Prod.*, 366, 132961, <https://doi.org/10.1016/j.jclepro.2022.132961>, 2022.

1198 Zhang, J., Liu, L., Zhao, Y., Li, H., Lian, Y., Zhang, Z., Huang, C., and Du, X.:  
1199 Development of a high-resolution emission inventory of agricultural machinery  
1200 with a novel methodology: A case study for Yangtze River Delta region, *Environ.*  
1201 *Pollut.*, 266, 115075, <https://doi.org/10.1016/j.envpol.2020.115075>, 2020.

1202 Zhang, L., Zhu, X., Wang, Z., Zhang, J., Liu, X., and Zhao, Y.: Improved speciation

1203 profiles and estimation methodology for VOCs emissions: A case study in two  
1204 chemical plants in eastern China, *Environ. Pollut.*, 291, 118192,  
1205 <https://doi.org/10.1016/j.envpol.2021.118192>, 2021a.

1206 Zhang, S. J., Wu, Y., Zhao, B., Wu, X. M., Shu, J. W., and Hao, J. M.: City-specific  
1207 vehicle emission control strategies to achieve stringent emission reduction targets  
1208 in China's Yangtze River Delta region, *J. Environ. Sci.*, 51, 75–87,  
1209 <https://doi.org/10.1016/j.jes.2016.06.038>, 2017a.

1210 Zhang, Q., Zheng, Y., Tong, D., Shao, M., Wang, S., Zhang, Y., Xu, X., Wang, J., He,  
1211 H., Liu, W., Ding, Y., Lei, Y., Li, J., Wang, Z., Zhang, X., Wang, Y., Cheng, J.,  
1212 Liu, Y., Shi, Q., Yan, L., Geng, G., Hong, C., Li, M., Liu, F., Zheng, B., Cao, J.,  
1213 Ding, A., Gao, J., Fu, Q., Huo, J., Liu, B., Liu, Z., Yang, F., He, K., and Hao, J.:  
1214 Drivers of improved PM<sub>2.5</sub> air quality in China from 2013 to 2017, *Proc. Natl.*  
1215 *Acad. Sci.*, 116, 24463-24469, doi:10.1073/pnas.1907956116, 2019a.

1216 Zhang, X. M., Wu, Y. Y., Liu, X. J., Reis, S., Jin, J. X., Dragosits, U., Van Damme, M.,  
1217 Clarisse, L., Whitburn, S., Coheur, P., and Gu, B. J.: Ammonia emissions may be  
1218 substantially underestimated in China, *Environ. Sci. Technol.*, 51, 12089–12096,  
1219 [10.1021/acs.est.7b02171](https://doi.org/10.1021/acs.est.7b02171), 2017b.

1220 Zhang, Y., Bo, X., Zhao, Y., and Nielsen, C. P.: Benefits of current and future policies  
1221 on emissions of China's coal-fired power sector indicated by continuous emission  
1222 monitoring, *Environ. Pollut.*, 251, 415-424,  
1223 <https://doi.org/10.1016/j.envpol.2019.05.021>, 2019b.

1224 Zhang, Y., Zhao, Y., Gao, M., Bo, X., and Nielsen, C. P.: Air quality and health  
1225 benefits from ultra-low emission control policy indicated by continuous emission  
1226 monitoring: a case study in the Yangtze River Delta region, China, *Atmos. Chem.*  
1227 *Phys.*, 21, 6411–6430, <https://doi.org/10.5194/acp-21-6411-2021>, 2021b.

1228 Zhao, Y., Wang, S., Nielsen, C. P., Li, X., and Hao, J.: Establishment of a database of  
1229 emission factors for atmospheric pollutants from Chinese coal-fired power plants,  
1230 *Atmos. Environ.*, 44, 1515-1523, <https://doi.org/10.1016/j.atmosenv.2010.01.017>,  
1231 2010.

1232 Zhao, Y., Zhang, J., and Nielsen, C. P.: The effects of recent control policies on trends

1233 in emissions of anthropogenic atmospheric pollutants and CO<sub>2</sub> in China, *Atmos.*  
1234 *Chem. Phys.*, 13, 487-508, 10.5194/acp-13-487-2013, 2013.

1235 Zhao, Y., Qiu, L. P., Xu, R. Y., Xie, F. J., Zhang, Q., Yu, Y. Y., Nielsen, C. P., Qin, H.  
1236 X., Wang, H. K., Wu, X. C., Li, W. Q., and Zhang, J.: Advantages of a city-scale  
1237 emission inventory for urban air quality research and policy: the case of Nanjing,  
1238 a typical industrial city in the Yangtze River Delta, China, *Atmos. Chem. Phys.*,  
1239 15, 12623–12644, <https://doi.org/10.5194/acp-15-12623-2015>, 2015.

1240 Zhao, Y., Mao, P., Zhou, Y., Yang, Y., Zhang, J., Wang, S., Dong, Y., Xie, F., Yu, Y.,  
1241 and Li, W.: Improved provincial emission inventory and speciation profiles of  
1242 anthropogenic non-methane volatile organic compounds: a case study for Jiangsu,  
1243 China, *Atmos. Chem. Phys.*, 17, 7733–7756,  
1244 <https://doi.org/10.5194/acp-17-7733-2017>, 2017.

1245 Zhao, Y., Xia, Y., and Zhou, Y.: Assessment of a high-resolution NO<sub>x</sub> emission  
1246 inventory using satellite observations: A case study of southern Jiangsu, China,  
1247 *Atmos. Environ.*, 190, 135-145, <https://doi.org/10.1016/j.atmosenv.2018.07.029>,  
1248 2018.

1249 Zhao, Y., Yuan, M., Huang, X., Chen, F., and Zhang, J.: Quantification and evaluation  
1250 of atmospheric ammonia emissions with different methods: a case study for the  
1251 Yangtze River Delta region, China, *Atmos. Chem. Phys.*, 20, 4275–4294,  
1252 <https://doi.org/10.5194/acp-20-4275-2020>, 2020.

1253 Zhao, Y., Huang, Y., Xie, F., Huang, X., and Yang, Y.: The effect of recent controls on  
1254 emissions and aerosol pollution at city scale: A case study for Nanjing, China,  
1255 *Atmos. Environ.*, 246, 118080, <https://doi.org/10.1016/j.atmosenv.2020.118080>,  
1256 2021.

1257 Zheng, B., Zhang, Q., Tong, D., Chen, C., Hong, C., Li, M., Geng, G., Lei, Y., Huo,  
1258 H., and He, K.: Resolution dependence of uncertainties in gridded emission  
1259 inventories: a case study in Hebei, China, *Atmos. Chem. Phys.*, 17, 921–933,  
1260 <https://doi.org/10.5194/acp-17-921-2017>, 2017.

1261 Zheng, B., Tong, D., Li, M., Liu, F., Hong, C., Geng, G., Li, H., Li, X., Peng, L., Qi, J.,  
1262 Yan, L., Zhang, Y., Zhao, H., Zheng, Y., He, K., and Zhang, Q.: Trends in China's

1263 anthropogenic emissions since 2010 as the consequence of clean air actions,  
1264 Atmos. Chem. Phys., 18, 14095–14111,  
1265 <https://doi.org/10.5194/acp-18-14095-2018>, 2018.

1266 Zheng, B., Cheng, J., Geng, G., Wang, X., Li, M., Shi, Q., Qi, J., Lei, Y., Zhang, Q.,  
1267 and He, K.: Mapping anthropogenic emissions in China at 1 km spatial  
1268 resolution and its application in air quality modeling, *Sci. Bull.*, 66, 612–620,  
1269 <https://doi.org/10.1016/j.scib.2020.12.008>, 2021.

1270 Zheng, J., Zhang, L., Che, W., Zheng, Z., and Yin, S.: A highly resolved temporal and  
1271 spatial air pollutant emission inventory for the Pearl River Delta region, China  
1272 and its uncertainty assessment, *Atmos. Environ.*, 43, 5112–5122,  
1273 [10.1016/j.atmosenv.2009.04.060](https://doi.org/10.1016/j.atmosenv.2009.04.060), 2009.

1274 Zheng, J. J., Jiang, P., Qiao, W., Zhu, Y., and Kennedy, E.: Analysis of air pollution  
1275 reduction and climate change mitigation in the industry sector of Yangtze River  
1276 Delta in China, *J. Clean. Prod.*, 114, 314–322,  
1277 <https://doi.org/10.1016/j.jclepro.2015.07.011>, 2016.

1278 Zhou, Y., Zhao, Y., Mao, P., Zhang, Q., Zhang, J., Qiu, L., and Yang, Y.: Development  
1279 of a high-resolution emission inventory and its evaluation and application  
1280 through air quality modeling for Jiangsu Province, China, *Atmos. Chem. Phys.*,  
1281 17, 211–233, <https://doi.org/10.5194/acp-17-211-2017>, 2017.

1282

1283 **Figure captions**

1284 Figure 1. Emission trends, underlying social and economic factors. Coal consumption  
1285 is achieved by Chinese Energy Statistics (National Bureau of Statistics, 2016-2020).  
1286 The GDP, population, and vehicle population data come from the National Bureau of  
1287 Statistics, (2016-2020). Data are normalized by dividing the value of each year by  
1288 their corresponding value in 2015.

1289 Figure 2. Anthropogenic emissions by sector and year. The species include (a) SO<sub>2</sub>, (b)  
1290 NO<sub>x</sub>, (c) CO, (d) AVOCs, (e) NH<sub>3</sub>, (f) PM<sub>10</sub>, (g) PM<sub>2.5</sub>, (h) BC, and (i) OC. Emissions  
1291 are divided into five sectors: power, industry, transportation, residential, and  
1292 agriculture.

1293 Figure 3. Changes in emissions by sector and year. The species include (a) SO<sub>2</sub>, (b)  
1294 NO<sub>x</sub>, (c) CO, (d) AVOCs, (e) NH<sub>3</sub>, (f) PM<sub>10</sub>, (g) PM<sub>2.5</sub>, (h) BC, and (i) OC. The 2015  
1295 emissions are subtracted from the emission data for each year to represent the  
1296 additional emissions compared to 2015 levels.

1297 Figure 4. The city-level emissions and spatial distribution include (a) SO<sub>2</sub>, (b) NO<sub>x</sub>, (c)  
1298 AVOCs, (d) PM<sub>2.5</sub>, and (e) NH<sub>3</sub>; and (f) the proportions of emission by different  
1299 regions for 2015 and 2019. The blue line indicates the Yangtze River. The map data  
1300 provided by Resource and Environment Data Cloud Platform are freely available for  
1301 academic use (<http://www.resdc.cn/data.aspx?DATAID=201>), © Institute of  
1302 Geographic Sciences & Natural Resources Research, Chinese Academy of Sciences.

1303 Figure 5. Difference in the spatial distribution of major pollutant emissions between  
1304 2015 and 2019 for (a) SO<sub>2</sub>, (b) NO<sub>x</sub>, (c) PM<sub>2.5</sub>, and (d) AVOCs. The black circles  
1305 represent the locations of top 10 emitters for corresponding species in each panel. The  
1306 blue line indicates the Yangtze River.

1307 Figure 6. The ratios of BVOCs to AVOCs emissions in July: (a) 2015, (b) 2017, and (c)  
1308 2019.

1309 Figure 7. Comparison of interannual trends with MEIC, EDGAR, and ground-based  
1310 observations: (a) SO<sub>2</sub> and (b) NO<sub>x</sub> (NO<sub>2</sub>).

1311 Figure 8. Comparison of Jiangsu emissions for 2017 with MEIC and An et al. (2021).  
1312 The air pollutants from left to right are SO<sub>2</sub>, NO<sub>x</sub>, VOCs, NH<sub>3</sub>, and PM<sub>2.5</sub>,  
1313 respectively.

1314 Figure 9. Contributions of individual measures to emission reductions in SO<sub>2</sub>, NO<sub>x</sub>,  
1315 VOCs, and PM<sub>2.5</sub> for 2015-2017 (the left column) and 2017-2019 (the right column).

1316 Figure 10. The monthly averages of (a) PM<sub>2.5</sub> and (b) MDA8 O<sub>3</sub> from CMAQ  
1317 simulation and ground observation for January, April, July and October from 2015 to  
1318 2019. The slopes of linear regressions in the panels indicate the annual variation rates  
1319 for corresponding species.

1320 Figure 11. The concentration changes during 2015-2017 and 2017-2019 from CMAQ  
1321 for (a) PM<sub>2.5</sub> and (b) O<sub>3</sub> (VEMIS and VMET: meteorological conditions and  
1322 emissions fixed at 2017 level, respectively).

1323

1324 **Tables**

1325 **Table 1 Annual emissions of BVOCs and AVOCs and the ratios of BVOCs to**  
 1326 **AVOCs.**

	Year	January	April	July	October	Annual
BVOCs (Gg)	2015	0.0020	8.1	38.0	3.9	150.0
	2016	0.0017	8.5	51.4	2.8	188.1
	2017	0.0023	9.4	58.7	2.8	212.7
	2018	0.0020	9.1	55.5	3.5	204.3
	2019	0.0017	6.9	53.4	4.1	193.2
AVOCs (Gg)	2015	131.3	102.8	101.8	104.0	1348.3
	2016	131.2	102.3	101.3	103.6	1346.4
	2017	123.4	97.0	96.0	98.2	1342.9
	2018	131.6	102.5	101.6	103.8	1306.0
	2019	127.7	99.4	98.4	100.6	1271.1
BVOCs/AVOCs ( $\times 10^{-2}$ )	2015	0.0	7.9	37.3	3.8	11.1
	2016	0.0	8.3	50.7	2.7	14.0
	2017	0.0	9.7	61.2	2.9	15.8
	2018	0.0	8.9	54.6	3.4	15.6
	2019	0.0	6.9	54.3	4.1	15.2

1327

1328

1329

1330

1331

1332

1333

1334

1335

1336

1337

1338

1339 **Table 2 Air pollutant emissions in Jiangsu and comparison with previous studies**

Data source		Annual air pollutant emissions (Gg·yr <sup>-1</sup> )						
		SO <sub>2</sub>	NO <sub>x</sub>	AVOCs	NH <sub>3</sub>	CO	PM <sub>10</sub>	PM <sub>2.5</sub>
2014	Li et al. (2018)	1002	1315	1560	544	12667	1761	779
2015	This study	627	1411	1348	468	7735	711	491
	Official emission statistics <sup>a</sup>	835	1068				655	
	MEIC	626	1646	2143	544	9059	595	444
	REAS	649	1343	2063	611	10980	827	622
	EDGAR	957	1693	2178	488	7157	814	573
	Sun et al. (2018)	1230	1700	2000		13780		
	Zhang et al. (2017)				703			
Yang et al. (2021a)	613	1285	1911	354	7711	781	617	
2016	This study	580	1391	1346	452	7397	687	475
	Official emission statistics	579	634				798	
	MEIC	468	1586	2128	532	8191	516	388
	EGGAR	905	1641	2126	453	6902	771	536
	Simayi et al. (2019)			2024				
	Yang et al. (2019) <sup>b</sup>		1245					
2017	This study	416	1331	1343	434	7305	676	468
	Official emission statistics	384	500				626	
	MEIC	315	1538	2132	528	7731	492	367
	EDGAR	876	1614	2116	432	6636	744	513
	An et al. (2021)	619	1165	2056	1093	17309	1440	404
2018	This study	374	1198	1306	430	7252	670	462
	Official emission statistics	316	497				526	
	MEIC	336	1456	1999	484	6513	365	272
	EDGAR	892	1653	2147	414	6813	751	517
	Gao et al. (2022)	210	830	3000	530	9950	310	260



2019	This study	296	1122	1271	422	7163	565	411
	Official emission statistics	226	333				242	
	MEIC	311	1414	1983	455	6380	351	263

1340 <sup>a</sup> The data were taken from Department of Ecology and Environment of Jiangsu  
 1341 Province (<http://sthjt.jiangsu.gov.cn/col/col83555/index.html>).

1342 <sup>b</sup> An estimate with the “top-down” methodology, in which the emissions were  
 1343 constrained with satellite observation and inverse modelling.

1344

1345

1346

1347

1348

1349

1350

1351

1352

1353

1354

1355

1356

1357

1358

1359

1360

1361

1362

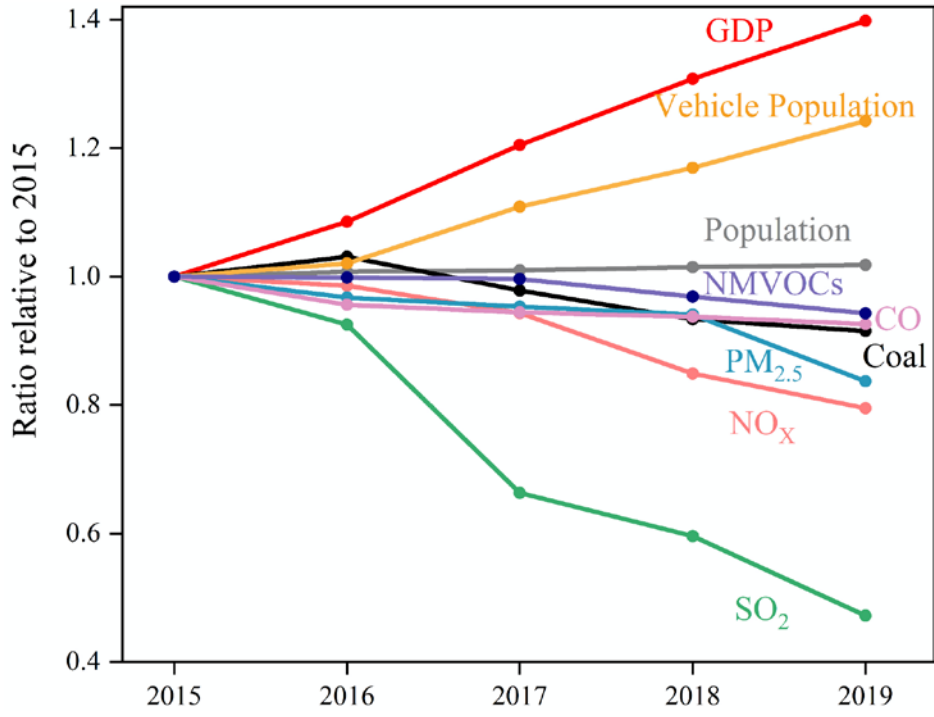
1363

1364

1365

1366

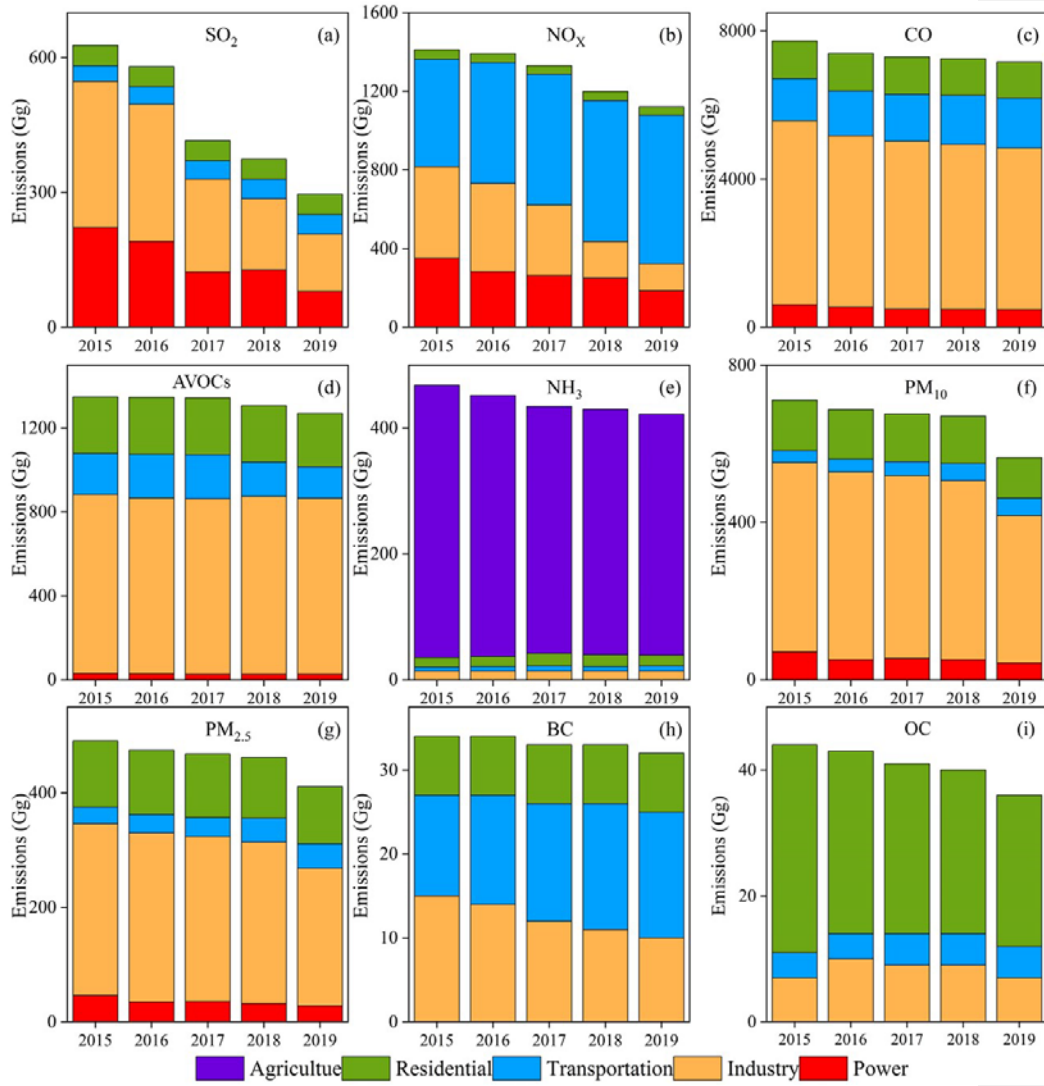
1367 **Figure 1**



1368  
1369  
1370  
1371  
1372  
1373  
1374  
1375  
1376  
1377  
1378  
1379  
1380  
1381

1382 **Figure 2**

1383



1384

1385

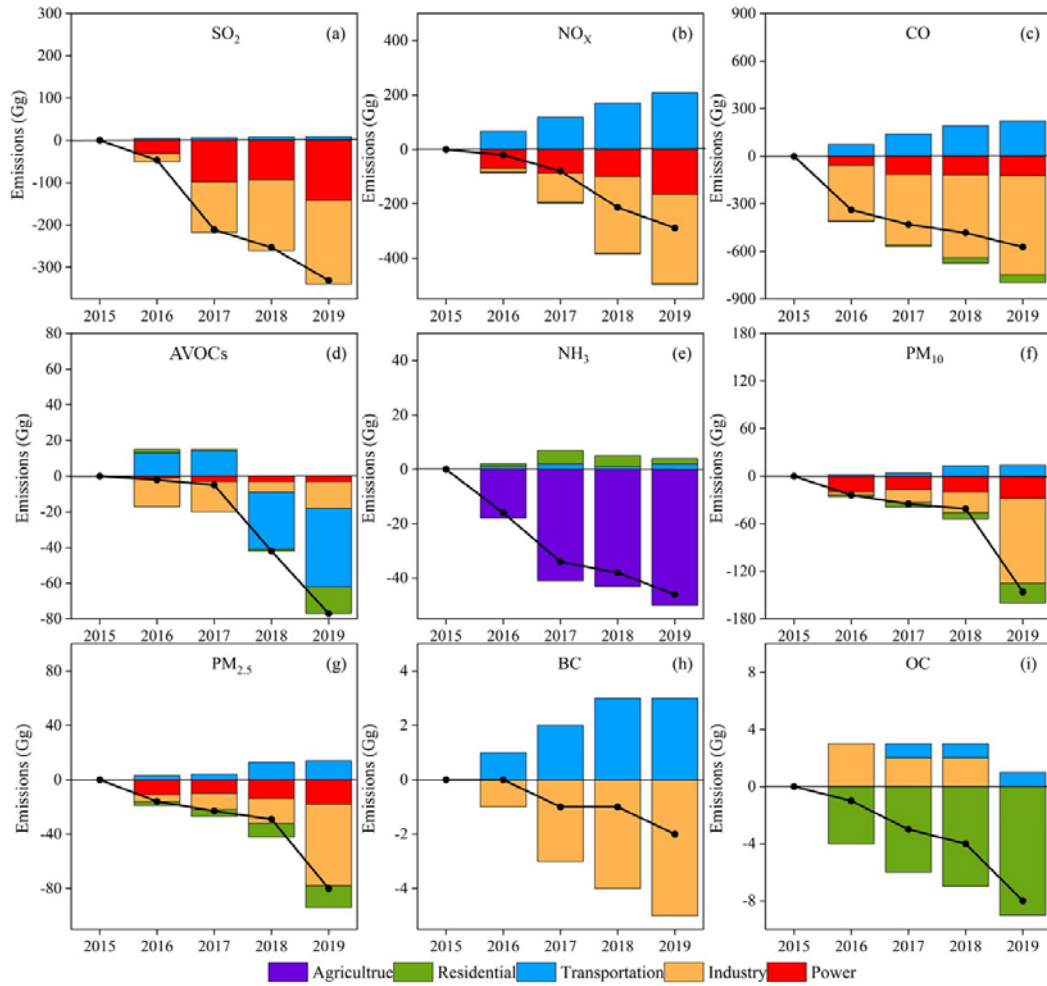
1386

1387

1388

1389

1390 **Figure 3**



1391

1392

1393

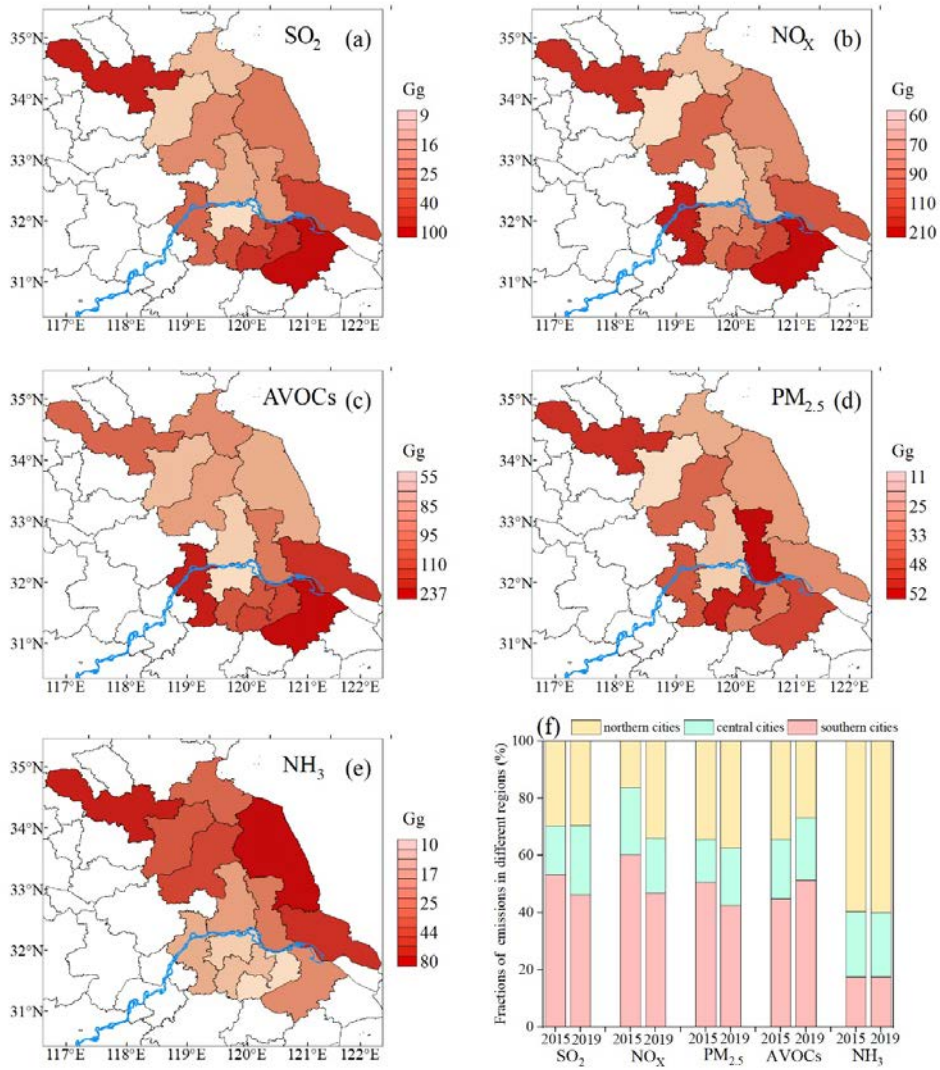
1394

1395

1396

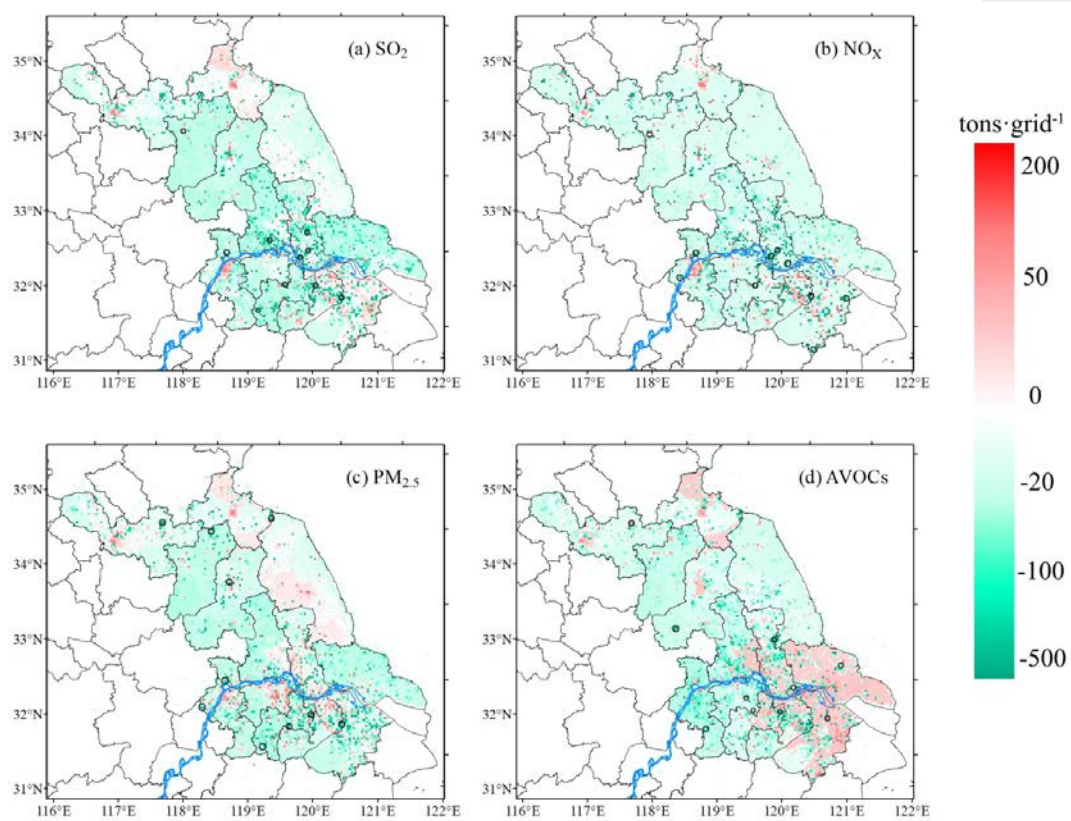
1397

1398 **Figure 4**



1399

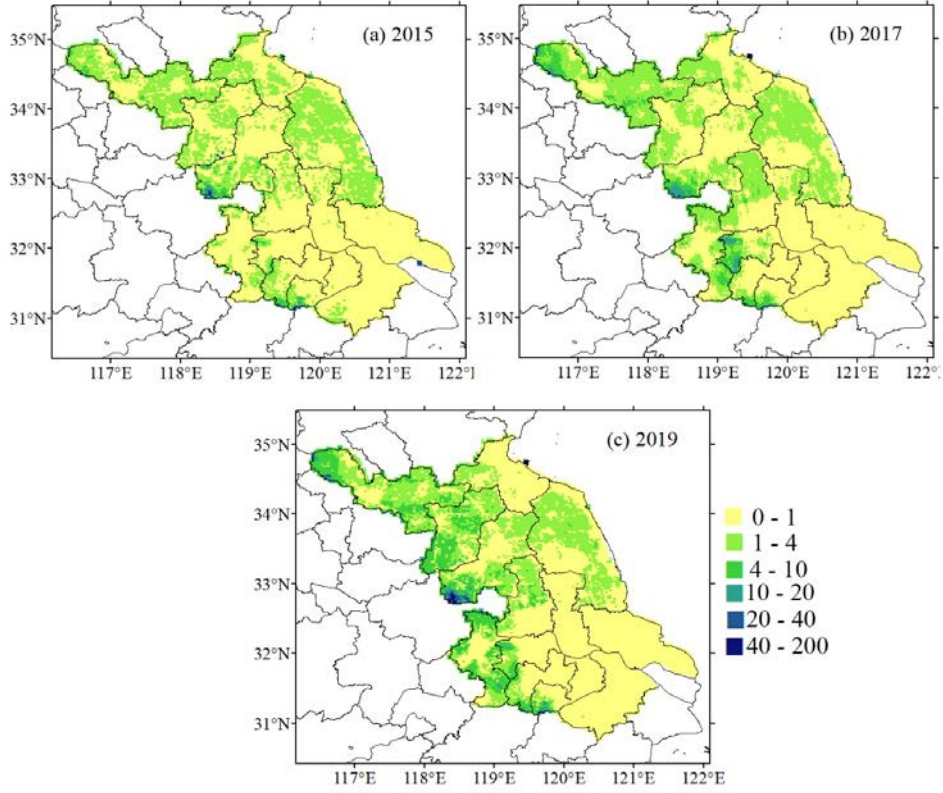
1400 **Figure 5**



1401

1402

1403 **Figure 6**



1404

1405

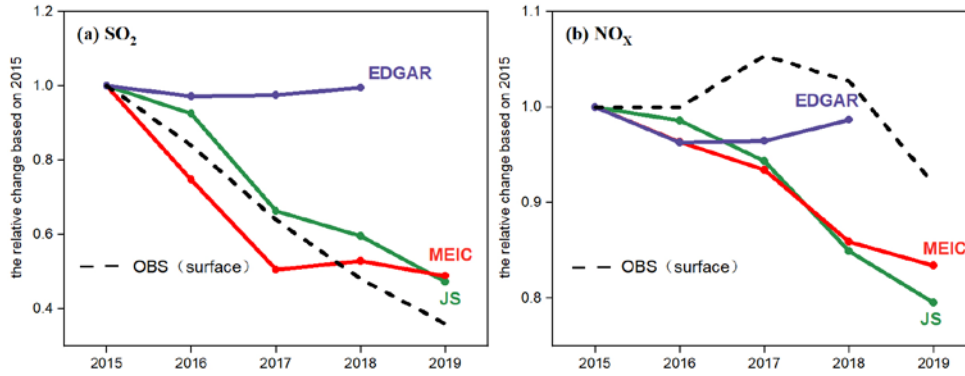
1406

1407

1408

1409

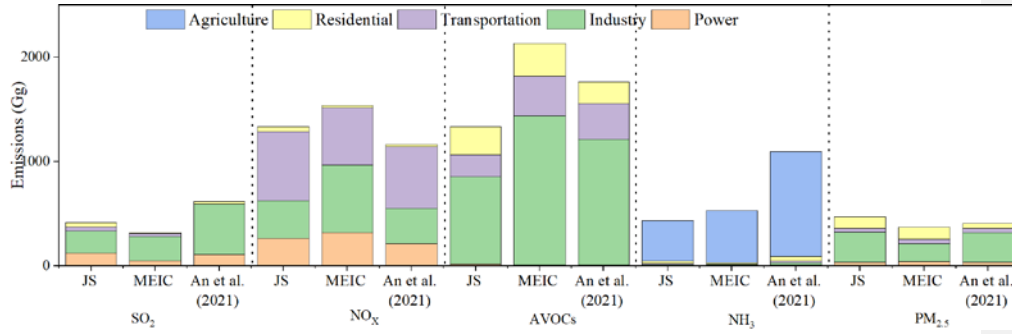
1410 **Figure 7**



1411  
1412  
1413  
1414  
1415  
1416  
1417  
1418  
1419  
1420  
1421  
1422  
1423  
1424  
1425  
1426  
1427  
1428  
1429  
1430  
1431  
1432

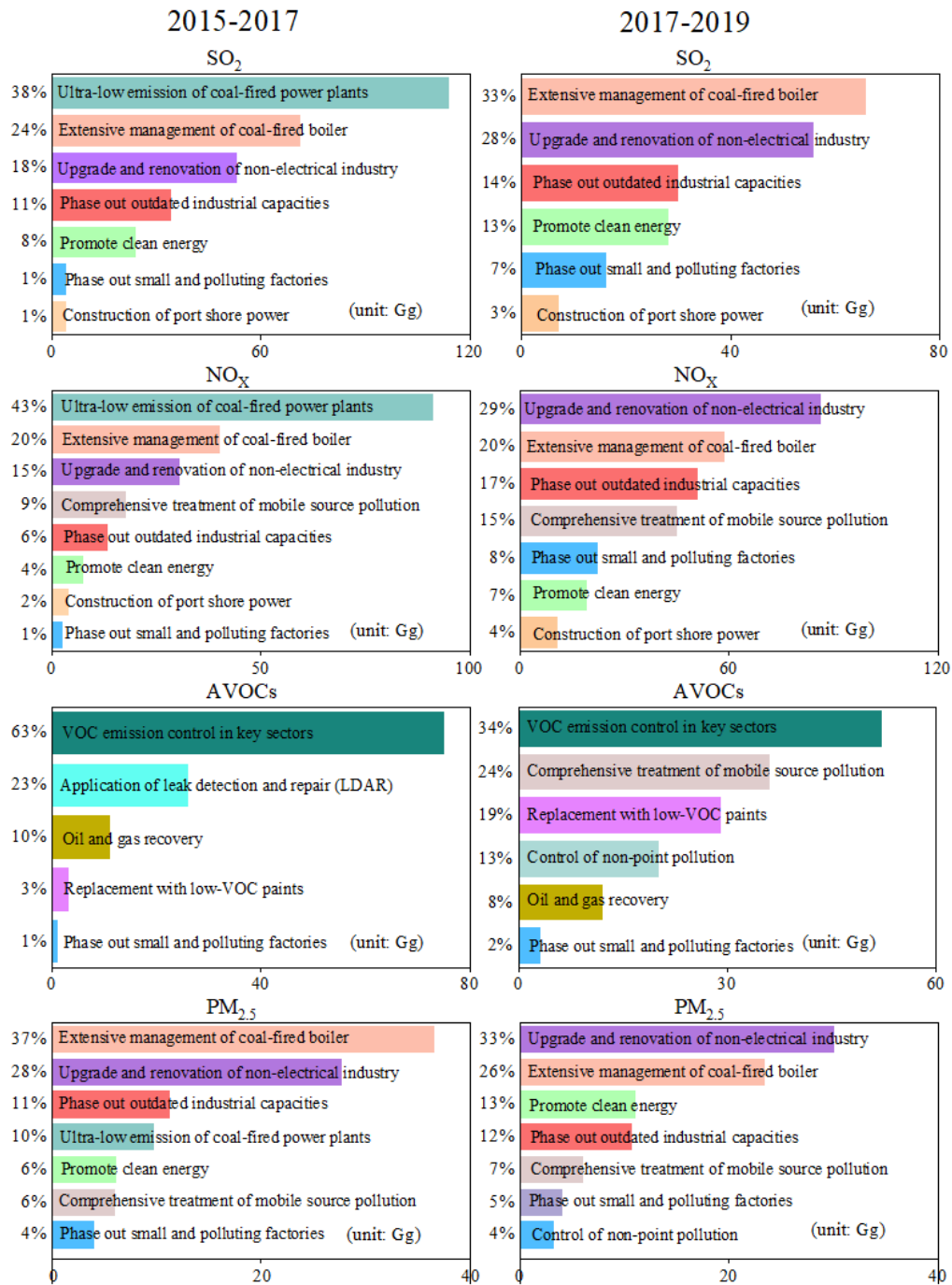


1433 **Figure 8**



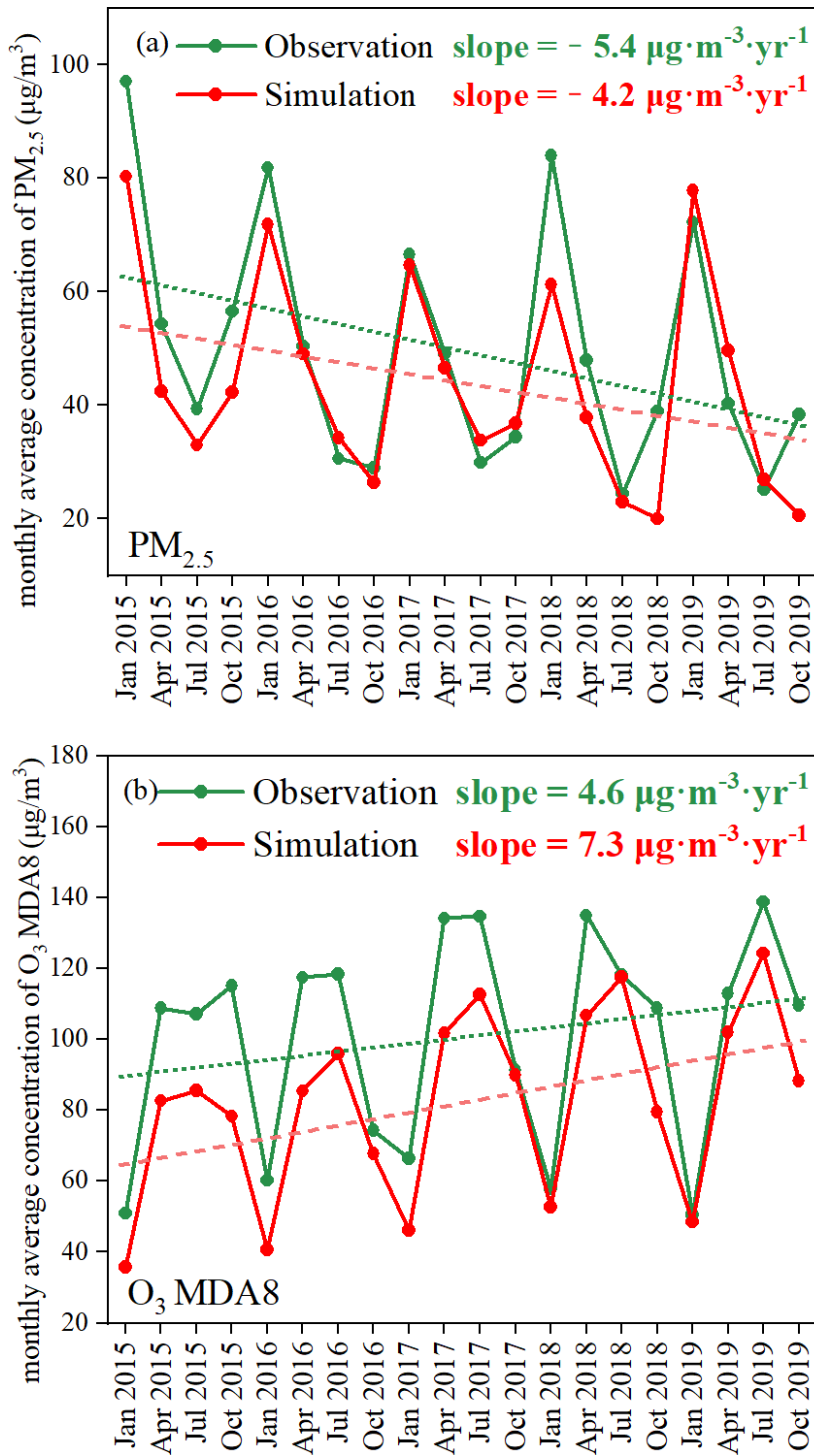
1434  
 1435  
 1436  
 1437  
 1438  
 1439  
 1440

1441 **Figure 9**



1442

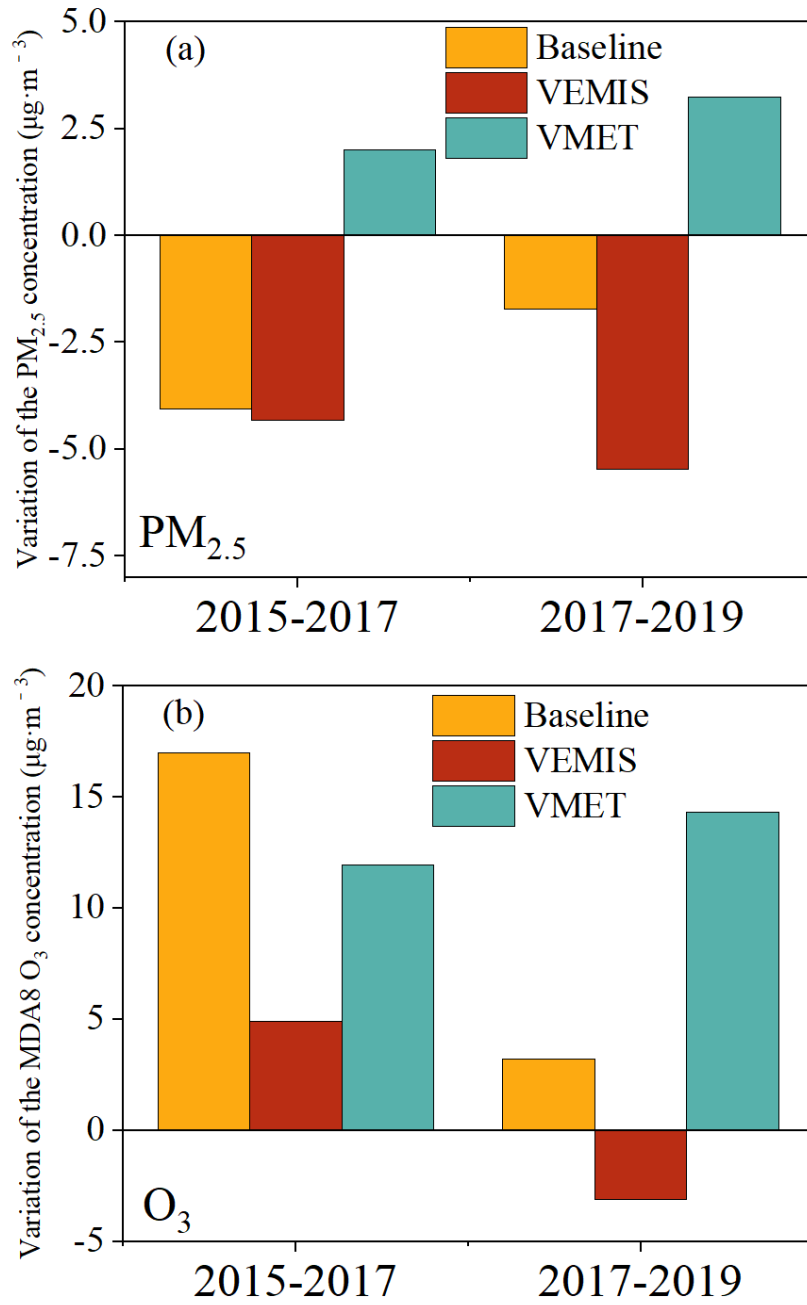
1443 **Figure 10**



1444

1445

1446 **Figure 11**



1447

1448